

**ATTEMPTS TO CLONE THE LIMULUS EPENDYMIN GENE,  
AND THE EFFECTS OF A HUMAN EPENDYMIN PEPTIDE  
ON HUMAN SHSY NEUROBLASTOMA CELLS**

A THESIS

Submitted to the Faculty

of the

WORCESTER POLYTECHNIC INSTITUTE

In partial fulfillment of the requirements for the

Degree of Master of Science

in

Biology and Biotechnology

by

---

Turkan Arca

May 5, 2005

APPROVED:

---

David S. Adams, Ph.D.  
Major Advisor  
WPI

---

Ronald Cheetham, Ph.D.  
Committee Member  
WPI

---

Daniel Gibson, Ph.D.  
Committee Member  
WPI

## ABSTRACT

This thesis was divided into two parts. The purpose of part I was to clone and sequence the full-length ependymin gene from the invertebrate *Limulus polyphemus*, or portions of the gene, and to use RT-PCR to determine whether expression of this gene increases during leg regeneration. PCR was chosen as the method for obtaining the gene due to the success our lab had previously characterizing several ependymin genes using this approach. Three sets of primers were designed based on the conserved domains between teleost fish and three invertebrate ependymin sequences. “Sea primers” were designed based on the nucleotide sequence of the sea cucumber *H. glaberrima* for each conserved domain, and these primers produced all four of the expected size amplicons with *Limulus* DNA, but surprisingly only one such band with the sea cucumber *Sclerodactyla briareus*. The consensus primers (con-primers) were designed based on the most conserved nucleotide among all known ependymin species at each particular position in the conserved domains. Primers designated “5-11 primers” were designed based on the absolutely conserved domains among the three known invertebrate ependymins. Neither con-primers nor 5-11 primers produced any bands of the expected size; this was true for both species of DNA. One very strong band was produced using “5-11” primer pair 6/10 with both species. One of the bands from this reaction from *Limulus* was cloned and sequenced, and showed a very strong homology (88% over 292 bp) with mouse FGF-14, a neurotrophic factor involved in mouse neurogenesis. The expression of this gene during leg regeneration will be tested in future experiments. *Limulus* GAPDH was also cloned and sequenced, and a genomic intron was identified for the first time in this study. This *Limulus* housekeeping gene will be used in future studies for gene expression comparisons.

The purpose of part two of this thesis was to study the up-regulation of growth-related genes induced by treatment of a human neuroblastoma SH-SY5Y cell line with a human ependymin peptide mimetic (hEPN-1), in an attempt to help provide a basis for using human EPN mimetics as therapeutics in stroke and neurodegenerative diseases. The sequence of this mimetic is derived from an area of human MERP-1 analogous to goldfish mimetic CMX-8933. The human mimetic was previously found to up-regulate growth related genes L-19, EF-2 and ATP Synthase in the mouse neuroblastoma cell line Nb2a (Saif, 2004). The expression levels of genes encoding ribosomal proteins and ribosomal RNA were studied using RT-PCR as hallmarks of proliferating cells. hEPN-1 was found to increase the expression of the nuclear-encoded ribosomal proteins S-19 and S-12, an average of 2.76 fold and 1.74 fold, with statistically significant p-values of 0.031 and 0.015 ( $<0.05$ ), respectively. The expression levels of nuclear-encoded 5.8S ribosomal RNA ( $p = 0.018$ ) and the mitochondrial-encoded 16S RNA ( $p = 0.046$ ) were found to be increased an average of 14.04 fold and 3.91 fold, respectively. Thus, human ependymin mimetic hEPN-1 appears to stimulate growth-related genes, a property which can be useful to regenerate neuronal tissue after injury.

## TABLE OF CONTENTS

ABSTRACT.....	2
TABLE OF CONTENTS.....	4
LIST OF FIGURES.....	5
LIST OF TABLES.....	6
ACKNOWLEDGEMENTS.....	7
BACKGROUND.....	8
THESIS PURPOSE.....	17
MATERIALS AND METHODS.....	18
RESULTS.....	27
DISCUSSION.....	51
BIBLIOGRAPHY.....	56

## LIST OF FIGURES

Figure 1. Phylogenetic Relationship of All Currently Characterized Ependymin and Ependymin-Related Sequences.....	12
Figure 2. Bioinformatic Alignments of Ependymin Amino Acid Sequences from Teleost Fish and Three Invertebrates.....	27
Figure 3. Relative Positions of 1-4 and 5-11 RT-PCR Primers on the <i>H. glaberrima</i> Ependymin Sequence.....	29
Figure 4. PCR Experiments with sea 1-4 Primers Using <i>Limulus</i> Genomic DNA at Various Annealing Temperatures.....	30
Figure 5. PCR Experiments with sea 1-4 Primers Using Sea Cucumber Genomic DNA at Various Annealing Temperatures.....	34
Figure 6. <i>Limulus</i> and Sea Cucumber PCR with con 1-4 Primers.....	36
Figure 7. <i>Limulus</i> and Sea Cucumber PCR with 5-11 Primers.....	37
Figure 8. PCR of <i>Limulus</i> Housekeeper Genes.....	39
Figure 9. BLAST of <i>Limulus</i> Clone-12 Against GenBank.....	40
Figure 10A. Sequence of <i>Limulus</i> GAPDH.....	41
Figure 10B. Alignment of <i>Limulus</i> Cloned GAPDH with the Genbank Entry for <i>Limulus</i> GAPDH.....	42
Figure 11. Bioinformatic Alignments of 39 Known Ependymin, or Ependymin-Related Proteins Characterized to Date.....	43
Figure 12. hEPN-1 Peptide Derived from h-MERP 1.....	47
Figure 13. RT-PCR Analysis of Growth-Related Ribosomal Protein Genes from hEPN-1 Treated (+) and Control (-) SH-SY5Y Human Neuroblastoma Cells.....	48
Figure 14. Quantitation of the Fold Upregulation of Growth-Related Genes Induced by hEPN-1.....	50

## LIST OF TABLES

Table 1. Summary of Cell Culture Reagent Volumes.....	19
Table 2. Summary of Genes Tested with Their Expected Amplicon Sizes.....	49
Table 3. Summary of Mean Fold Upregulation and Corresponding p-values.....	49

## ACKNOWLEDGEMENTS

First and foremost, I would like to express my greatest gratitude and thanks to my Major Advisor, Professor David Adams, for his outstanding advice and guidance throughout my thesis project. Without his immense help and support this thesis would have never been possible. I would like to thank him for taking me into his lab and giving me the greatest opportunity I have ever had in my academic life, which is to learn through his exceptional knowledge and experience. I have had the greatest honor of being trained by him in one-to-one sessions, and his time and patience were extremely valuable to me. My respect for him can not be explained by words. Every single conversation I have had with him led me to broaden my horizons and explore my limits further. Everything I have learned from him will stay with me throughout my life, and I will walk in my career with firm steps. My endless thanks go to him for making me appreciate science, and love and respect the profession once again, so that I can now have a better future. I would like to extend my sincere thanks to my committee members, Dr Daniel Gibson and Dr Ronald Cheetham for their valuable advice and optimism throughout my thesis program. I would like to thank to Dr Dan Gibson for providing the *Limulus* and sea cucumber tissues, as well as *Limulus* data and pictures, and for all his encouragement throughout the project. I also wish to thank to Sakina Saif, who helped me learn cell culture skills when I first joined the lab, and whose project I took over. Thanks also to Dr Elizabeth Ryder for her valuable consultation on statistical analysis, and to Ceremedix for partially funding the project. And finally I especially thank my family, my mom and dad, and my brother for their love and extreme support whenever I needed them. Thank you Mom and Dad for raising me the way I am, for always giving me the best of everything you possibly can, and for always believing in me. My love for you and my appreciation for what you have done *for* me is beyond words. And thank you, my brother, for being a ‘Big Brother’ to me at times, although you are the younger, and for not leaving me alone in the US. I started with *our* “America” dream, Dad. Now I am at the end.

## BACKGROUND

### Neurotrophic Factors

Neurotrophic factors (NTF's) are proteins of the central and peripheral nervous systems whose functions are to promote growth, development, and differentiation of neuronal and glial cells (Abe, 2000; Ikeda *et al.*, 2000). NTF's have a role in the normal maintenance and survival of neuronal cells after differentiation, and are involved in the protection and repair of mature neurons under pathological conditions (Hefti, 1997; Abe, 2000). Neurotrophic factors also stimulate neurite sprouting (Patel and McNamara, 1995), and promote axonal regeneration. NTF synthesis is known to be induced after ischemia, and the exogenous administration of NTF's was shown to protect the brain tissue from ischemic damage (Abe, 2000). Neural stem cells also exist in the mature mammalian brain, and as such they have the potential to compensate for lost neural functions due to injury (Abe, 2000). Because of their ability to control neural stem cell differentiation into certain neural populations (Abe, 2000), NTFs are being considered as potential therapeutic agents following brain injury.

During development, NTF's are secreted by target cells, and are then transported to the developing neuron's cell body via axonal retrograde transport. This NTF signal guides the growing axon of the developing neuron to reach the target tissue if it can receive sufficient signal. Therefore, many axons compete for a limited quantity of NTF's produced by the target cells, and neurons which fail to obtain a sufficient quantity will die by apoptosis. This process is thought to regulate synaptic plasticity (the number of neurons and neuronal connections made) during CNS development (Connor and Dragunow, 1998). Muscle cells, the target cells at the neuromuscular junction, also synthesize and secrete NTF's in a similar fashion. NTF's can also be secreted by surrounding glial cells in paracrine fashion, or by the neuronal cells themselves in an autocrine fashion.

Different classes of neurotrophic factors use different cell surface receptors. For example, the neurotrophin family of NTFs, which includes the Nerve Growth Factor (NGF), Brain-derived neurotrophic factor (BDNF), and Neurotrophins NT-2, NT-4/5 and NT-6, mainly

use tyrosine kinase (trk) receptors (Abe, 2000). NGF and BDNF are especially known to activate AP-1 transcription factor as part of their mechanism of action (Gaiddon *et al.*, 1996; Ip *et al.*, 1993), which in turn activates neuronal growth genes. The exact mechanism of action of NTFs is not yet elucidated.

## **Ependymin**

Ependymin (EPN) is a neurotrophic factor first discovered in the goldfish brain following a learning event (Shashoua, 1976; Shashoua and Moore, 1978). It was first localized to the 'zona ependyma' of the goldfish brain (Shashoua and Benowitz, 1977), and was later found to be synthesized in meninges (Hoffmann *et al.*, 1990) and secreted into the brain extracellular fluid (ECF) and cerebrospinal fluid (CSF), where it is predominately found.

### *EPN Molecular Features*

Ependymin is a 216 aa secreted glycoprotein that exists as a disulfide-linked dimer in the ECF of goldfish. It has a glycosylated  $\beta$  form and a non-glycosylated  $\gamma$  form; the gamma  $\gamma$  form has no major homologies to any known protein, except short 5-7 aa regions homologous to human N-CAM, to the fiber components of the extracellular matrix (ECM) such as laminin and fibronectin, and to intracellular tubulin (Shashoua, 1991). Ependymin (after activation by phosphorylation) can irreversibly polymerize into Fibrous Insoluble Polymers (FIPs) under reduced calcium conditions, such as the synapse following repeated neural firing or receiving convergent inputs from simultaneously firing neighbouring cells (Shashoua, 1988; Shashoua *et al.*, 1990). FIPs are insoluble in solutions that would dissolve other ECM components, which distinguishes EPN from other ECM components. EPN also has a carbohydrate moiety (glucuronic acid sulfate) with similar antigenicity to the cell surface glycoprotein HNK-1 (involved in cell-adhesion), and to the glycan epitopes of neural cell adhesion molecule (N-CAM) and myelin-associated glycoprotein (MAG) (Shashoua, 1991). EPN has many negatively charged residues (Adams *et al.*, 1996) which might confer to EPN its calcium binding ability.

EPN's N-glycosylation sites are rich in sialic acid residues which are also believed to contribute to the calcium binding ability (Ganss and Hoffmann, 1993).

### *EPN Functions and Mechanisms*

Ependymin is implicated in the formation of synaptic changes during the consolidation step of learning and in neuronal regeneration. Three types of behavioral experiments in fish (including classical conditioning and avoidance conditioning experiments), one behavioral experiment in mammals (T-maze learning in mice), and long-term potentiation studies in rat hippocampus, all implicate EPN's role in Long Term Memory formation (Shashoua, 1991). EPN was also shown to have a role in optic nerve regeneration in goldfish, where increased synthesis was observed during the regeneration process, and antisera to the C-terminal end of EPN blocked the sharpening of retinotectal projection (Shashoua and Schmidt, 1988).

Ependymin's FIP-forming property was suggested to be the underlying mechanism in its ability to generate synaptic plasticity at regions receiving simultaneous neighbouring inputs during LTM formation and neuronal regeneration (Shashoua, 1990). The sharpening process during neuronal regeneration is thought to involve FIP formation, serving as a suitable substrate for the regenerating axons to seek and grow on; this is supported by the observation that the ECM components themselves have been considered to have a role in synapse formation, since the regenerating motor axons of the neuromuscular junction would form presynaptic terminals at the synapse region on the basal lamina in the absence of a motor terminal (Shashoua and Schmidt 1988; Shashoua, 1990). Ependymin was also observed to act as a substrate for the outgrowth of axons from cultured goldfish retina (Schmidt *et al.*, 1991). Regarding EPN's proposed role as a substrate for regenerating axons, this could involve EPN's cell-adhesion moiety which is believed to direct the growth of central axons *in vitro* (Schmidt, 1995), and thus aid in axonal pathfinding. EPN was also shown to promote neurite outgrowth in neuroblastoma cell cultures (Shashoua, 1991).

The calcium binding ability of EPN is thought to help in regulating calcium homeostasis in brain (Shashoua, 1991). This might be beneficial especially after ischemic injury where the

excess calcium intake is associated with cytotoxicity. In vitro experiments using CMX-9236, a goldfish ependymin mimetic, indeed demonstrated the ability of the short peptide to chelate intracellular calcium and return it to normal levels following kainite/glutamate induced cytotoxicity; the same peptide was shown to have neuroprotective effects in an *in vivo* rat stroke model, where it significantly reduced the infarct volume (Shashoua *et al.*, 2003).

## **EPN Phylogeny**

The phylogenetic distribution of ependymin and ependymin-like molecules is diverse. To date, immunological studies have indicated that ependymin-like molecules might exist in the vertebrate brains of goldfish, chick, mouse, rat and human (Shashoua, 1991), and in neural tissues of an invertebrate *Aplysia* (Shashoua, 1990). EPN has so far been cloned in 7 orders of teleost fish including Cypriniformes, Clupeiformes, Siluriformes (catfish), Characiformes and Gymnotiformes (electric fish), Salmoniformes and Esociformes (Orti and Meyer, 1996). Cypriniformes include goldfish 1 and 2, carp, golden shiner, giant danio, and zebrafish, which represent “true” ependymins showing 91-95% homology to gf-1 protein (Adams *et al.*, 1996; Adams and Shashoua, 1994). Ependymin-related proteins (ERPs) have also been cloned from vertebrates other than fish, such as frog. Mammalian homologs of ependymin (MERP’s) have been identified in mouse (m-MERP 1 and 2), monkey, and in humans (human MERP-1) (Apostolopoulos *et al.*, 2001; Gregorio-King *et al.*, 2002). ERP’s were recently cloned in three invertebrates: sea cucumbers *Holothuria glaberrima*, and *Holothuria mexicana*, and sea urchin *Lytechinus variegatus*. The latter two were cloned as expressed tagged sequences (ESTs) (Suarez-Castillo *et al.*, 2004) using mRNA as starting material. So a higher ERP copy number in mRNA versus the genome may have facilitated its cloning success in these invertebrates. Figure 1 below shows the phylogenetic relationship of all ependymin and ependymin-related sequences identified so far (Suarez-Castillo *et al.*, 2004).

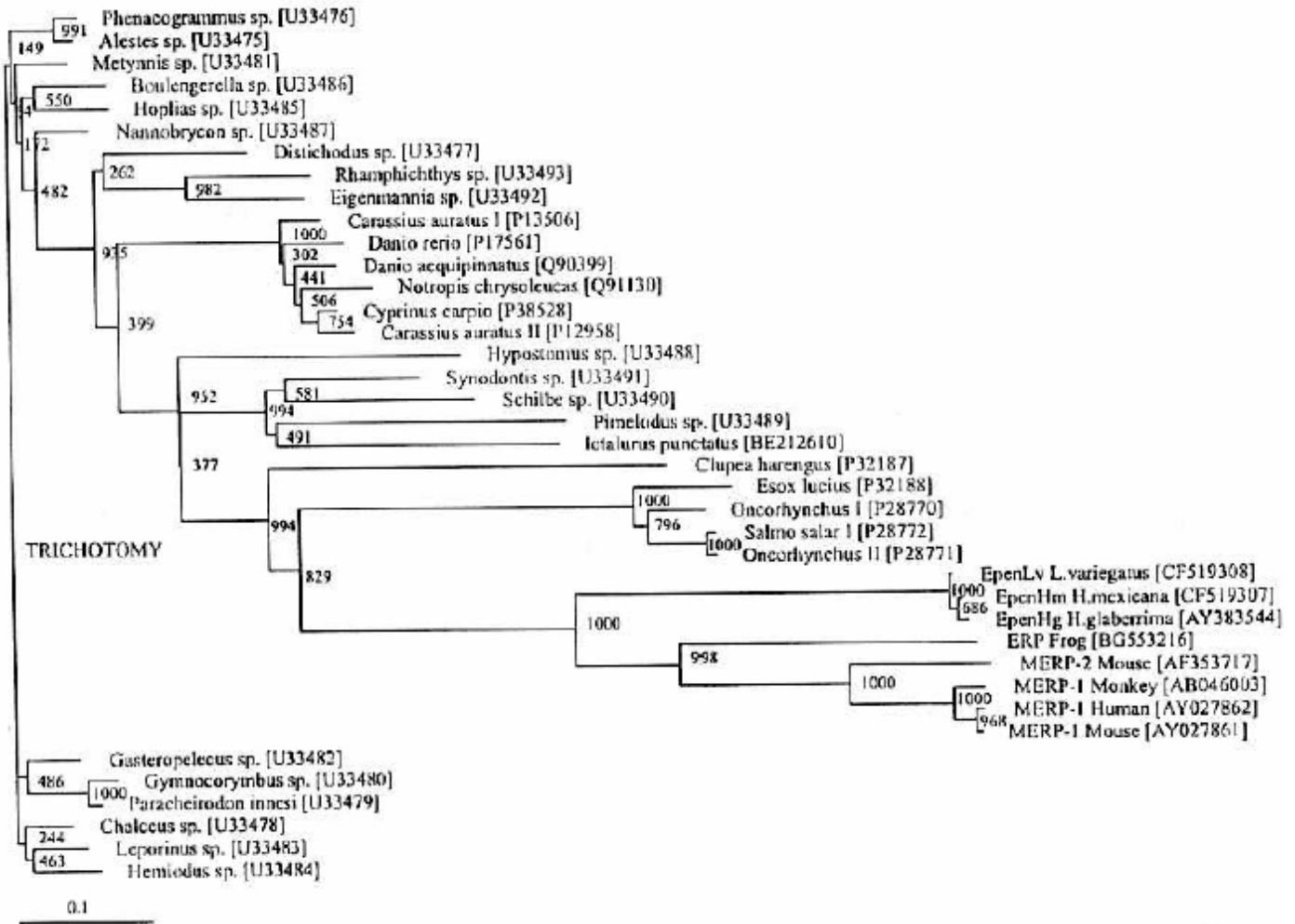


Figure 1- Phylogenetic Relationships of All Currently Characterized Ependymin and Ependymin-Related Sequences (Suarez-Castillo *et al.*, 2004).

## Human MERP-1

A human homolog of ependymin was discovered in CD34+ hematopoietic stem cells by differential display: A strongly expressed gene was identified in CD34+ cells from cord blood and bone marrow compared to CD34- cells of a more differentiated lineage. Subsequently, human MERP was cloned from a liver cDNA library, and this 1 kb cDNA, representing 224 aa, was mapped to the 7p14.1 chromosomal region. Three human MERP pseudogenes were also identified on separate chromosomes. Interestingly, human MERP is highly expressed in several

hematopoietic cell lines, malignant tissues, and malignant cell lines, so human MERP may function in cell growth. Human MERP was also highly expressed in non-hematopoietic tissues, such as brain, heart, skeletal muscle, prostate, testis and ovary, while moderate expression was observed in kidney and low expression in thymus, spleen, liver, placenta, lung, small intestine, and colon (with or without mucosal lining) (Apostolopoulos *et al.*, 2001; Gregorio-King *et al.*, 2002). It is particularly interesting to consider the low EPN expression in the colon of a healthy individual, since the human homolog of ependymin (although a partial cDNA) was first identified in a colon cancer tissue by its high expression, and was named UCC-1 (Upregulated Colon Cancer-1) (Nimmrich *et al.*, 2001).

### **Ependymin Mimetics and Stroke Therapy**

Because of their ability to regenerate brain tissue, NTFs have been considered as potential therapeutic agents for neurodegenerative diseases and stroke (Hefti, 1997). Because early experiments indicated full-length NTFs delivered i.v. did not efficiently cross the blood brain barrier (BBB), Ceremedix Inc. (Maynard, MA) currently focuses on designing short peptides to mimic the function of full-length NTFs.

Peptide mimetics CMX-8933 and CMX-9236 have sequences based on the goldfish EPN sequence. CMX-9236 was found to chelate intracellular calcium in a glutamate/kainate hippocampus *in vitro* model for stroke, and it was also found to reduce infarct volume in a rat stroke model *in vivo* (Shashoua *et al.*, 2003). Similarly, NGF and BDNF also show neuroprotective effects in rat stroke models when delivered intraventricularly to the brain. CMX-8933 and full-length ependymin were shown to use the MAPK signal transduction pathway to activate AP-1 transcription factor in mouse neuroblastomas (Adams *et al.*, 2003). AP-1 is known to be involved in the activation of neuronal growth genes, including NTFs themselves, and it also acts as a master-switch upstream of CREB to regulate LTM and synaptic plasticity (Sanyal *et al.*, 2002). Interestingly, NGF, BDNF, EGF and NT-3 are all known to activate AP-1 as part of their mechanism of action.

Both CMX-8933 and 9236 have recently been found to increase gene expression of antioxidants superoxide dismutase (SOD), catalase (CAT), and glutathione peroxidase (GPX) in rat brain and heart tissues *in vivo*, and in primary rat cortical cells *in vitro* (Shashoua *et al.*, 2004). Antioxidative therapy could be beneficial in treating diseases and conditions involving oxidative stress, such as neurodegenerative disorders, heart attacks, stroke, and aging (Chan and Kawase, 1998). The activation of SOD by CMX-8933 was shown to be dependent on the activation of AP-1 in mouse neuroblastoma cell cultures (Saif, 2004).

### **Ependymin and Regeneration**

Evidence exists that EPN may play a role in tissue regeneration during spinal cord injury. The zona ependyma of urodele amphibians was observed to undergo massive reorganization during spinal cord regeneration: “injury-reactive” ependymal cells showed changes in intermediate filament and fibronectin expression, the latter of which would significantly alter the composition of the ECM (O’Hara *et al.*, 1992). These processes are believed to be associated with a change of shape and outgrowth of ependymal cells during the regeneration process. In particular, ependymal cells will detach from their initial site, move towards the lesion site, proliferate and re-organize themselves at the lesion site in order to remodel the site. In order for this to occur, ependymal cells (normally epithelial) switch their intermediate filament expression from that of cytokeratin (characteristic of epithelial cells) to vimentin (characteristic of mesenchymal cells) (O’Hara *et al.*, 1992). While the ependymal cells migrate to the lesion site, they will secrete metalloproteinases to dissolve the ECM components for their ease of movement (Chernoff *et al.*, 2003; Chernoff 1996), and they will also secrete fibronectin to form the matrix base for its movement (O’Hara *et al.*, 1992). Once the ependymal cells reach the lesion site, they will re-organize and re-model the site, after which they will re-epithelialize. Interestingly, fibrous glial cells also disappear during spinal cord regeneration of adult urodeles, which help “open up” space for the migration of ependymal cells to the lesion site. In adult mammals, however, these fibrous glial cells are known to be the primary injury-reactive cells, and they will form a scar tissue at the lesion site, which might then prevent ependymal cells migrating into the site inhibiting the regeneration process (O’Hara *et al.*, 1992; Chernoff *et al.*, 2003). These

ependymal cells could also act as a buffer at the site of injury through their calcium uptake which will protect neurons from the harmful effects of calcium cytotoxicity (Chernoff *et al.*, 2003).

Injury-reactive ependymal cells are thought to act as ‘neural stem cells’ during regeneration, where they will produce fibroblast growth factor FGF and respond to EGF in order to proliferate, both of which are characteristics of neuronal stem cells (Chernoff *et al.*, 2003). Even in the intact urodele spinal cord, ependymal cells will retain their embryonic character, which is thought to occur via the continued contact of ependymal cells with the basal lamina (Chernoff, 1996). Differentiated ependymal cells in the adult mammalian brain are considered to be the possible candidates as sources of neuronal progenitor cells (Johansson *et al.*, 1999). To accomplish this role, ependymal cells might switch back and forth between differentiated and undifferentiated stages, and could therefore be potentially useful for recovery after ischemic injury (Abe, 2000).

Self-organization of ependyma also occurs during the spinal cord regeneration in teleost fish (Anderson *et al.*, 1986), and morphological changes in ependymal cells have also been observed in the regenerating spinal cord of the lizard tail (Egar *et al.*, 1970). Ependymal cells are also thought to contribute to the regeneration process by producing NTFs; ependymal extracts were indeed found to extend the survival of CNS neurons *in vitro* (Chernoff, 1996). So perhaps one of the NTFs produced by ependymal cells is ependymin.

### **Invertebrates as Models for Tissue Regeneration**

Invertebrates, such as sea cucumbers, are well known for their regenerative capacities (Garcia-Ararras and Greenberg, 2001). Recently, an ependymin like protein was identified from a sea cucumber, *H. glaberrima*, where it was found to be over-expressed during intestine regeneration (Suarez-Castillo *et al.*, 2004). The horseshoe crab itself is a good model for regeneration because of its well-known ability to regenerate its limbs, such as its legs and tail (Clare *et al.*, 1990).

## *Limulus EPN*

In horseshoe crab, reactivity to anti-ependymin antibody SHEILA was observed in the juvenile ganglion (nervous tissue), with heavier staining in neuropils, and in extracellular spaces around axons, intracellular membrane complexes and connective tissue. At an earlier embryo stage, no staining was observed in neuronal tissue (Barroso, 1999). These observations imply that *Limulus* EPN might exist, with a role in horseshoe crab growth and development, during which its expression varies temporally. More recently, positive staining with SHEILA antibody was observed in the blood cells of an adult wounded male (Costigan and Gallant, 2004). In addition, injection of SHEILA antibody was shown to block the growth of a regenerating leg (Baroffio, 2000).

Our lab has also cloned the 3' end of *Limulus* 'ependymin' using PCR primers derived against goldfish EPN (Cruikshank *et al.*, 1993). The short sequence shows 94% homology to goldfish EPN-1 (Ibid). To assess ependymin's biological role in the horseshoe crab might bring new insights into how the protein might function in the regeneration of non-neuronal tissue.

## THESIS PURPOSE

The goal of Part 1 of this thesis was to clone the ependymin gene, or portions thereof, from *Limulus polyphemus* DNA, and to determine whether its expression increases during leg regeneration. Earlier data from the Gibson lab indicated that various tissues show immunoreactivity against antibody SHEILA induced against the C-terminal end of goldfish EPN-1, and injection of this antibody in a regenerating leg blocks its growth. Thus an EPN-like molecule may indeed exist in *Limulus* that functions in regeneration. PCR was chosen as the experimental approach due to our lab's earlier success using PCR to clone the 3' end of a gene showing very high homology with goldfish EPN-1. The recent identification of ependymin-like genes in three other invertebrates (Suarez-Castillo *et al.*, 2004) provided the main basis for our primer design. Characterizing the gene from the horseshoe crab, one of the oldest living organisms on earth (over three hundred million years without significant changes in body plan) would deepen our phylogenetic knowledge of ependymin. The horseshoe crab provides a good model for studying tissue regeneration.

The goal of part 2 was to study the up-regulation of growth-related genes by a human ependymin mimetic (hEPN-1) in a human neuroblastoma SH-SY5Y cell line. The sequence of this mimetic is derived from an area of human MERP-1 analogous to goldfish mimetic CMX-8933, and was previously found to up-regulate growth related genes L-19, EF-2 and ATP Synthase in the mouse neuroblastoma cell line Nb2a (Saif, 2004). The current thesis will test the ability of hEPN-1 to stimulate growth in human cells by studying the expression levels of growth related genes using RT-PCR. Since increased ribosomal protein and ribosomal RNA expression is a hallmark of cell proliferation (Raska *et al.*, 2004), the gene expression of S-19, S-12, L-19, and L-11 ribosomal proteins, and 5.8S and 16S ribosomal RNAs will be studied in particular. This thesis will help understand the biological effects of human ependymin mimetics on human cells, and help provide a basis for using human EPN mimetics as therapeutics.

## MATERIALS AND METHODS

### Human Neuroblastoma Cell Culture

#### *Cell Properties and ATCC Recommendations*

This thesis represents the first culture of a human neuroblastoma cell line in our lab, so the culture methods are more detailed than usual. SH-SY5Y was originally established in 1970 from a metastatic bone tumor in a neuroblastoma patient, and the source of the tumor was identified as the brain tissue. The cells were purchased from American Type Culture Collection (ATCC) (Catalog No. CRL-2266). SH-SY5Y cells (sometimes abbreviated SHSY) grow as a mixture of suspension and adherent cells with an epithelial morphology. They are also reported to grow in clusters with multiple, short and fine neurites, and to aggregate, form clumps and float. The ATCC recommended subculturing ratio was 1:20 to 1:50, with a doubling time of 48 hours. Recommendations also included growth in a 5% CO<sub>2</sub> incubator at 37°C, with medium renewal every 4-7 days.

#### *Preparation of Complete Medium*

The medium used for subculturing was as recommended by ATCC in a 1:1 mixture of DMEM and F-12 (Dulbecco's Modified Eagle's Medium with non-essential amino acids and Ham's F-12 Nutrient Mixture). DMEM/F-12 (ATCC) contained 2.5 mM L-glutamine, 15 mM HEPES, 0.5 mM sodium pyruvate and 1200 mg/L sodium bicarbonate. The medium was supplemented with Fetal Bovine Serum (FBS) (to 10%) and Gentamycin (to 5 µg/ml). After adding the latter two components, the complete medium was sterilized using a 0.2 µm filtration unit with vacuum pump. The medium was stored at 4°C, and pre-warmed in a 37°C water bath before each use.

### *Cell Plating, Subculturing and Maintenance*

The ATCC SHSY cell vial arrived on dry ice. The 1 ml vial contents were thawed for 2 minutes in a 37°C water bath and transferred to a 15 ml conical tube. 9 ml of pre-warmed complete medium was added, and the cells were centrifuged for 5 minutes at medium speed in a clinical centrifuge (25°C). The cell pellet was re-suspended in 1 ml pre-warmed medium then added to 15 ml pre-warmed medium in a vented T-75 flask. The flask was incubated in a 5% CO<sub>2</sub> incubator at 37°C overnight.

The next day, the medium containing floating cells was removed, and the remaining attached cells were rinsed with fresh pre-warmed medium to remove trace amounts of DMSO from the original ATCC freezing medium. After aspirating the wash, fresh 15 ml of pre-warmed medium was immediately added to the adherent cells. The medium containing floating cells was centrifuged as above, and the supernatant containing toxic DMSO was removed. The pellet was resuspended in 1 ml medium, and transferred to the T-75 flask. A similar strategy was used when thawing vials of frozen cells prepared during this project.

When the T-75 flask reached 65-85% confluency, the adherent cells were scraped into their medium containing the suspended cells. The whole flask content was then transferred into a 15 ml or 50 ml conical tube and centrifuged to pellet the cells. The supernatant was removed, and the pellet was resuspended in fresh medium before transferring to new T-75 flasks containing fresh medium. The cells were split approximately 1:20 and fed two-three times a week.

<b>Flask Type</b>	<b>Total Volume in Flask During Culture (ml)</b>
T-25	6
T-75	15
T-150	25

**Table 1. Summary of Cell Culture Media Volumes.**

### *Cell Freezing*

When SHSY cells were to be frozen, the cell pellet obtained from one T-150 flask was resuspended in 1 ml of freezing medium containing DMSO (Gibco) and placed into a cryovial. The vial was usually stored at  $-80^{\circ}\text{C}$  overnight (or 1-2 days) to ensure a slow cell freezing, and then transferred to a liquid nitrogen tank.

### *SHSY Morphology*

The SH-SY5Y cells have a pyramidal appearance with short multiple neurites, while some of them look elongated with no neurites. The floating cells were observed to have a round morphology.

## **Culture Treatments**

Human EPN peptide-1 (hEPN-1) with the sequence KQCSKMTLTQPWDP was purchased from Abbott Laboratories, and was stabilized in a solution of 1% BSA at a final peptide concentration of 1 mg/ml. A T-150 flask grown to 60-80% confluency was treated with a final concentration of 1  $\mu\text{g/ml}$  hEPN-1 for 3 hours at  $37^{\circ}\text{C}$ . One or two T-150 flasks were used for each experimental group (control and drug treated).

## **Extraction of Total Cellular RNA**

Total cellular RNA was extracted from SHSY cells using a guanidine isothiocyanate/phenol extraction procedure (adapted from Clontech's Atlas Pure Total RNA Labeling System protocol; section "RNA Isolation from Cultured Cells). If two T-150 flasks were used for each experimental group, then these flasks were pooled together. A plastic cell scraper was used to dislodge the cells from the flask, and the entire content was poured into a 50 ml conical tube.

The cells were collected by centrifugation in a clinical centrifuge (25°C) at medium speed. The supernatant was discarded except for a little volume which was used to transfer the cells into a 1.5 ml eppendorf tube on ice (hereafter all steps were performed on ice, and centrifugations were at 4°C). The tubes were microfuged for 30 sec at maximum speed to pellet the cells. The entire supernatant was discarded. The pellet from two T-150 flasks now exists in one eppendorf tube.

In order to lyse the cells, 500 µl of denaturing solution was added to each pellet representing either the drug-treated or non-treated samples. The cells were thoroughly resuspended by pipeting up and down and vortexing, and then they were incubated on ice for 5-10 minutes. After microfuging for 5 minutes at 4°C at maximum speed (13K) to pellet cell debris, 500 µl of the cleared supernatant was transferred into a 2 ml eppendorf tube.

Phenol extraction was performed by adding 1000 µl of buffer-saturated phenol (4°C) into each tube and vortexing for 1 min for a thorough extraction. The tube was incubated on ice for 5 min, after which 300 µl chloroform (25°C) was added. The tube was vortexed again for 1 min and incubated on ice for 5 more minutes. The tubes were microfuged for 10 minutes at 4°C at 13K, and the upper aqueous phase (about 500 µl) was aliquotted into a 1.5 ml eppendorf tube.

For isopropanol precipitation, a double volume of 4°C isopropanol (usually 1 ml) was added to the aqueous phase in the eppendorf tube. The tubes were gently inverted to mix, avoiding vortexing. After incubating on ice for 10 minutes, the tubes were microfuged for 15 minutes at 4°C at 13K. After all the supernatant was discarded, the white RNA pellet should be quite visible at this stage. The RNA pellet was washed by adding 500 µl of -20°C, 70-100% ethanol, and vortexing briefly. The tubes were further microfuged for 5 minutes at 4°C at 13K, and the supernatant was discarded, being careful to not lose the loose RNA pellet. The pellets were air-dried overnight with a Kimwipe® over the open cap of the tube.

The dry pellet was dissolved in 40 µl of RNase free distilled water. If the pellets from more than one tube of the same sample were to be combined, the final tube must contain a total

of 40  $\mu$ l. Usually the tube was warmed in hand or in a 50°C water bath to facilitate dissolution, and the tubes were briefly microfuged before OD analysis.

The RNA concentration was determined by absorbance at 260 nm. 1  $\mu$ l of RNA solution was added into 1000  $\mu$ l dH<sub>2</sub>O, and the OD was taken at 260 nm. The RNA concentration was calculated using the following formula: RNA concentration in  $\mu$ g/ $\mu$ l = OD value x 42  $\mu$ g/ml x 1000 dilution factor x 1 ml/1000  $\mu$ l. A typical yield was about 120  $\mu$ g from two T-150 flasks (3  $\mu$ g/ $\mu$ l in 40  $\mu$ l). The RNA solution was then diluted to a 1  $\mu$ g/ $\mu$ l final concentration in a 0.5 ml eppendorf tube, and stored at -80°C. The RNA was thawed on ice before use in RT-PCR experiments.

### **Reverse Transcriptase-Polymerase Chain Reaction (RT-PCR)**

RT-PCR was performed using the RETROscript Kit from Ambion, or using SuperTaq Polymerase and MMLV (Ambion) to supplement the kit.

#### *RT*

A 20  $\mu$ l RT reaction was set up in a 0.5 ml tube as follows: 2  $\mu$ g RNA (2  $\mu$ l of 1  $\mu$ g/ $\mu$ l RNA), 2  $\mu$ l of 50  $\mu$ M oligo(dT) primer, and 8  $\mu$ l dH<sub>2</sub>O. The tube contents were briefly microcentrifuged, and the RNA was denatured at 85°C for 3 minutes in a PCR thermocycler. The tubes were immediately placed on ice to prevent RNA renaturation, briefly microfuged and put back on ice. 2  $\mu$ l of 10X RT Buffer, 4  $\mu$ l of 2.5 mM dNTPs and 1  $\mu$ l 10U/ $\mu$ l RNase Inhibitor were added into each tube. Usually this was prepared as a master mix, and 7  $\mu$ l was allocated into each tube. After adding 1  $\mu$ l of 100 U/ $\mu$ l MMLV-RT, the tubes were flicked to mix, microcentrifuged briefly, and immediately placed into the PCR machine. Reverse transcription was allowed to take place for 60 min at 42°C, followed by a 10 min denaturation step at 92°C. cDNA samples were either used immediately for PCR, or stored at -20°C.

## *PCR*

Each PCR reaction was set up in a 0.5 ml eppendorf tube containing the following (added in the order indicated): 2.5  $\mu$ l 10  $\mu$ M sense primer, 2.5  $\mu$ l 10  $\mu$ M antisense primer, 39.6  $\mu$ l of a master mix (containing 5  $\mu$ l of 10X PCR Buffer, 2.5  $\mu$ l of 2.5 mM dNTP's and 32.1  $\mu$ l dH<sub>2</sub>O), 5  $\mu$ l of the cDNA template from the above RT reaction, and finally 0.4  $\mu$ l of 5U/ $\mu$ l Taq polymerase to reach a final volume of 50  $\mu$ l. The tubes were flicked to mix and microfuged briefly before taking to the PCR machine.

The PCR reaction conditions for the human ependymin experiments were as follows: 2 min initial denaturation at 94°C; 30 cycles of amplification including a 30 sec denaturation at 94°C, 30 sec annealing at 55°C, and 40 sec elongation at 72°C; and a final 5 min elongation at 72°C.

## *Gel Electrophoresis*

PCR reactions were analyzed on 2.5% agarose gels in 1X TAE buffer, containing 1  $\mu$ g/ml ethidium bromide. 10  $\mu$ l of PCR sample was mixed with 1  $\mu$ l of 10X DNA sample buffer (containing 0.1X dyes) in an eppendorf tube, microfuged briefly, and mixed by pipeting up and down before loading onto the gel. Gel electrophoresis was carried out at 60 V for 1 hour for small units, and 2 hours for larger units. Gels were visualized under a UV trans-illuminator, photographed using a digital camera, and the band intensities were quantified using Scion Image Software (NIH).

## *Gel Normalizations*

For human ependymin experiments, the samples were normalized to the GAPDH 'housekeeper'. 2-3  $\mu$ l of GAPDH PCR samples (control and drug treated) were analyzed by gel electrophoresis to determine the signal ratio between the two samples. This ratio was then used to adjust the volumes of the drug treated and control samples for the rest of the experiment.

### *Statistical Analysis of Fold Upregulations*

The fold up-regulation of a particular amplicon for drug treated versus control samples was determined using Scion Image software (NIH) to produce band OD data. Fold up-regulation values from a number of independent experiments were then used to obtain a mean fold up-regulation value. The p values were determined using the EXCEL t-test for paired two sample for means: In order for the program to calculate the statistical significance of the mean fold up-regulation relative to 1, the log of the fold up-regulation values were entered as the first variable input range, and was compared to the log of 1 as the second input range (control).

### **Sequence Alignments**

For the bioinformatics alignments, the Megalign (Lasergene) ClustalV program was used.

### **Tissue Extraction from *Limulus***

Sperm tissue was obtained from a mature male horseshoe crab by Dr. Dan Gibson (Department of Biology and Biotechnology, WPI) as follows: The cover to the gill flaps (operculum) was reflected to reveal the genital pores. Sperm issued through these pores were collected using a 3 mm syringe and placed dry in an eppendorf tube. Samples were used for DNA extraction immediately, or were stored at -80°C.

### **DNA Extraction from *Limulus***

DNA extraction was performed by Dave Adams (Department of Biology and Biotechnology, WPI). Spooled sperm DNA was obtained as follows: *Limulus* sperm cells were microfuged for 5 min at 2000 rpm, and the supernatant was discarded. The cell pellet was dissolved in a mix of 100 µl 10 mg/ml Proteinase K and 10 ml DNA Lysis Buffer (50 mM Tris-HCl pH 8.0, 400 mM NaCl, 2 mM EDTA, 1.0% SDS), then transferred into a JA-20 centrifuge tube. The tube was incubated overnight at 37°C on a nutator. The next day, 10 ml (an equal

volume) of Phenol/Chloroform/Isoamyl alcohol solution (25:24:1) was added, and the JA-20 tube was incubated at room temperature overnight on a nutator. The following day, it was centrifuged in a J218 Beckman for 5 minutes at 10K rpm at 4°C. The upper aqueous phase was transferred into a fresh JA-20. A double volume (20 ml) of 100% ethanol was added, and the tube was swirled to mix. The tube was incubated at room temperature for 5 minutes, after which the High Molecular Weight white DNA strands were removed using a glass Pasteur pipette (spooling). Spooled DNA was rinsed by dipping it into 100% ethanol in a 15 ml plastic conical tube. The DNA was then placed in a fresh 15 ml conical tube and air-dried. Finally the DNA was dissolved in 2 ml of TE buffer. The concentration was determined by OD at 260 nm, assuming 1 OD = 50 µg/ml ds DNA.

### **Sea Cucumber Tissue Extraction**

The sea cucumber *Sclerodactyla briareus* (Catalog Number: 1870, [http://www.mbl.edu/marine\\_org/catalog/catalog.php](http://www.mbl.edu/marine_org/catalog/catalog.php)) was kindly provided gratis by Mr. Edward Enos of the Department of Marine Resources, Marine Biological Laboratory, 7 Water Street, Woods Hole, MA 02543. The tissue extraction was performed by Dr. Dan Gibson (WPI) as follows: Animals were obtained in filtered natural sea water. They were slit longitudinally and pinned open to view the gonad and the gut. Male gonad tissue was extracted using stainless steel tweezers, and placed dry in an eppendorf tube. DNA extraction was performed by Professor Dave Adams (WPI) as described above.

### ***Limulus* and Sea Cucumber PCR**

Each *Limulus* PCR reaction was performed as described above, except the 5 µl of template included either 2.55 µg of spooled *Limulus* sperm DNA or 2.17 µg of sea cucumber DNA. The primer concentrations for *Limulus* C-reactive protein were 10 µM instead of the usual 50 µM due to the strong signal.

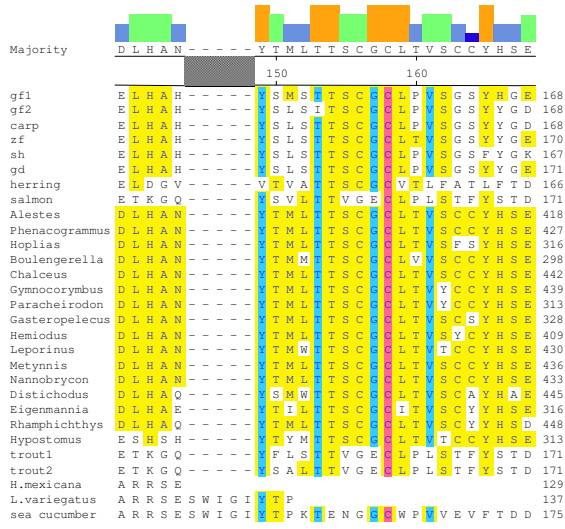
For a serial PCR reaction: 5  $\mu$ l of the first PCR reaction was used as template for a second PCR reaction. 10  $\mu$ l of PCR reaction was mixed with 1  $\mu$ l of 10X sample buffer (containing 10X dye and 50% glycerol) prior to analysis on agarose gels as described previously.

### **Polyacrylamide Gel Electrophoresis**

Sometimes PCR samples were analyzed on PAGE when higher resolution was required. Electrophoresis was performed in a BRL V-16 unit. One large and one small glass plate, two 1.5 mm plastic side spacers and a bottom spacer were cleaned with ethanol before set-up. The gel was prepared by adding 8.3 ml of 30% Acrylamide solution (4°C), 1 ml of 50X TAE, and 1 ml of 5% ammonium persulfate solution (4°C) (in this order) into a 50 ml conical tube and filling up to 50 ml with distilled water. Immediately before pouring, the gel between the glass plates, 50  $\mu$ l of 100% TEMED catalyst (4°C) was added, and the contents were gently mixed by inverting the tube. The gel was immediately poured between the glass plates and the 1.5 mm comb was placed in. The gel was allowed to solidify for 1 hour at room temperature, or usually Saran®-wrapped overnight. The next day the comb was removed and the gel was pre-run for 15-20 minutes at 150-200V in 1X TAE buffer in a vertical V-16 electrophoresis unit. Without further delay, the samples were loaded (10  $\mu$ l PCR reaction mixed with 1  $\mu$ l of 10X loading dye) using a V-16 tip, and the gel was electrophoresed for 2 hour at 150V. The gel was post-stained for 20 minutes with 1 $\mu$ g/ml EtBr in dH<sub>2</sub>O, and visualized under a UV trans-illuminator.

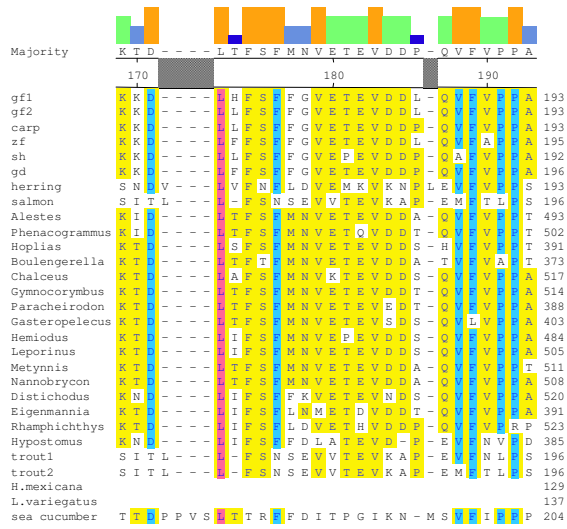


**IDENTITY ALIGNMENT**  
(residues 144-168: gf-1 reference)



Panel B

**IDENTITY ALIGNMENT**  
(residues 169-193: gf-1 reference)



Panel C



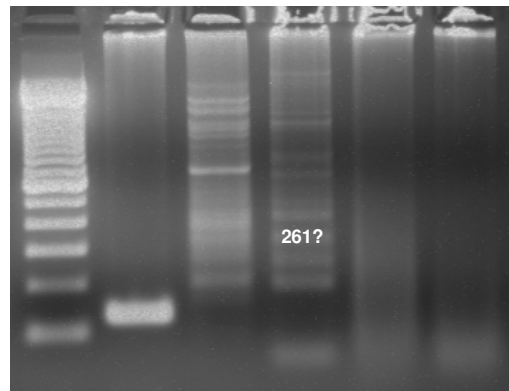
### ***Limulus* PCR with Sea Primers**

Figure 4 shows PCR experiments using *Limulus* genomic DNA at various annealing temperatures. The primer pairs used were 1 and 3 (1/3), 1/4, 2/3, and 2/4 for both sets (sea or con primers). Expected amplicon sizes are denoted in bp underneath each lane for each primer pair. *Limulus* C-reactive protein (CRP) was used as a positive control during all PCR reactions with *Limulus*. An elongation time of 1 min at 72°C was used throughout all experiments, with a range of annealing temperatures.

## **Limulus PCR, non-serial, Annealing temp 55°C, elongation 1 min**

Sea primers

100 bp crp 1/3 1/4 2/3 2/4



127 150 261 105 216 bp

**Figure 4A – *Limulus* Non-Serial PCR at 55°C Annealing Temperature.** Only a faint 261mer seems to appear at its expected size using primers 1/4. Note the strong positive control CRP signal indicating the *Limulus* DNA is intact, and the PCR conditions are working.

**Limulus PCR, non-serial,  
Annealing temp 37°C, elongation 1min**

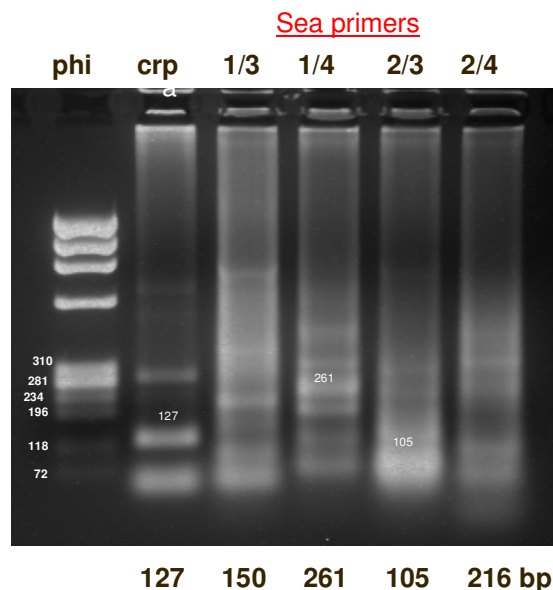


**Figure 4B – Limulus Non-Serial PCR at 37°C Annealing Temperature.**  
A 105mer starts to appear at this lower annealing temperature for pair 2/3, as well as a 261mer for pair 1/4.

**Limulus PCR, serial, Annealing temp 37°C,  
elongation 1 min**

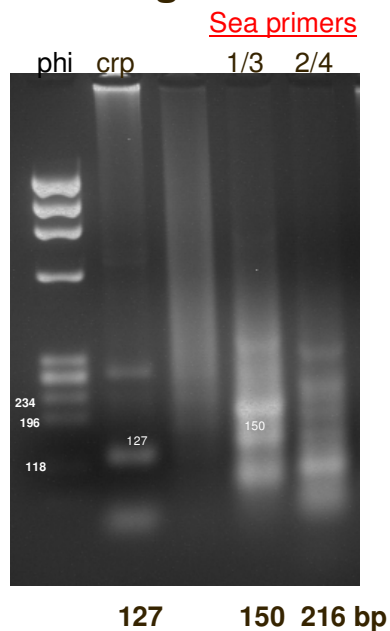
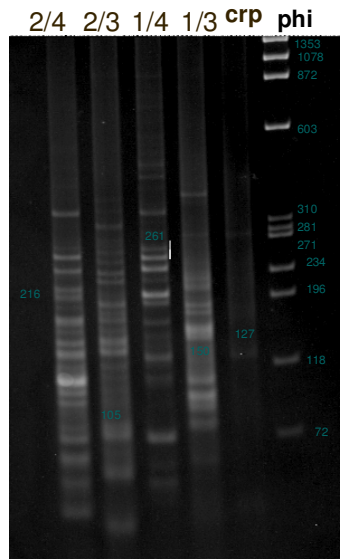


**Figure 4C - Serial PCR at a 37°C Annealing Temperature.** Note the new appearance of a 150mer for pair 1/3, that was absent in the non-serial reaction in Panel B. Still no bands were observed in the 216 bp range for reaction 2/4.

## Limulus PAGE

Sea primers

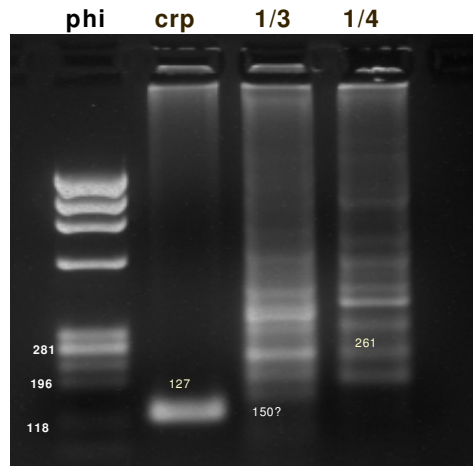


216 105 261 150 127 bp

**Figure 4D – PAGE Resolution of the Reactions From Panels B and C.**  
A better resolution PAGE finally brings a 216mer for pair 2/4.

## Limulus PCR, Annealing temp 58°C, elongation 1min

sea primers



127 150 261 bp

**Figure 4E - Non-Serial PCR With an Annealing Temperature of 58°C.** A higher annealing temperature of 58°C was used to try to eliminate the appearance of multiple bands in each lane. The 150mer was not as strong at this higher annealing temperature (see Discussion for possible interpretation).

Non-serial PCR using a 55°C annealing temperature (Panel A) showed a very strong 127 bp band for the positive control C-reactive protein (CRP) whose sequence was obtained directly from Genbank. Thus the *Limulus* DNA is intact and pure enough to generate clean PCR signals, and the PCR reagents work well. The reaction using primers 1 and 4 produced a possible 261 bp amplicon near the expected size, however several other bands were also seen in this lane, so this could represent non-specific amplification. Panel B shows non-serial PCR using a 37°C annealing temperature. In this case, the 261mer for set 1/4 remains visible as before, but also a very strong 105mer is visible for set 2/3. Panel C represents a serial PCR using a 37°C annealing temperature, in which a portion of the reactions in the previous panel were used as template for a new round of PCR. In the past in our lab this technique has proved effective for amplifying low abundance bands. However no improvement was seen in any of the reactions, except a faint 150mer for pair 1/3. Panel D represents a PAGE analysis of the reactions from Panels B and C. PAGE provides far more resolution than agarose gels. In this case, bands in the expected size ranges were observed for all primer pairs tested (216 bp for 2/4, 105 bp for 2/3, 261 bp for 1/4, 150 bp for 1/3), however many bands were observed in each lane, so again this may only represent non-specific amplification. The annealing temperature was increased to 58°C in Panel E in an attempt to make the reactions more stringent, however no significant improvement was observed. The relatively weaker appearance of 150mer as compared to the earlier reactions at lower annealing temperatures was notable (see Discussion).

### **Sea Cucumber PCR**

Because sea cucumber ependymin-related protein had previously been cloned (Suarez-Castillo *et al.*, 2004) we decided to increase our chances of obtaining successful EPN PCR

reactions by testing our primer sets against *S. briareus* genomic DNA (Figure 5). Panel A shows the results of non-serial (left side) and serial (right side) PCR at an annealing temperature of 37°C, as determined to be “optimum” from the earlier PCR reactions with *Limulus*. The non-serial PCR showed a 150 bp band of the expected size for set 1/3, which amplified much stronger when using serial PCR (white arrow in the figure). The 105 bp band was also observed following PAGE (Panel B). Attempts were made to clone and sequence this 105 bp band for verification, but initial attempts failed to clone it.

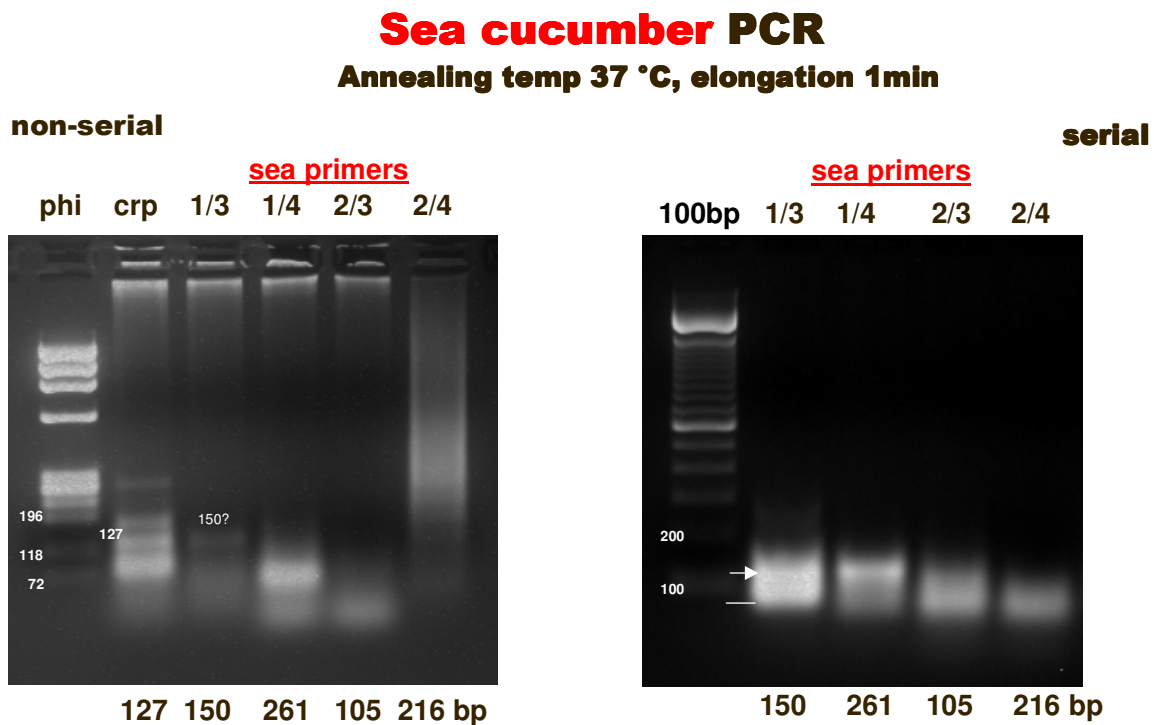
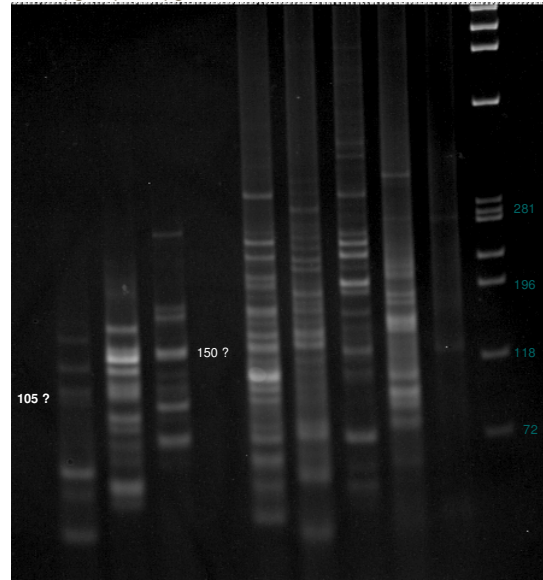


**Figure 5A – Sea Cucumber PCR at an Annealing Temperature of 37°C.** Only a faint 150mer seems to appear at its expected size with the non-serial reaction, and more strongly with the serial reaction. 1/4 primer pair gives two strong bands of different sizes with the serial and non-serial reactions. The other two primer pairs do not give any discrete bands under these “optimum” reaction conditions.

## PAGE **Sea cucumber**

### sea primers

2/3 1/4 1/3



105 261 150 bp

**Figure 5B - PAGE Analysis of Reactions from Panel 5A.** The gel gives a strong amplicon closer to the expected size of 150mer, and a faint amplicon of what could represent a 105mer. Primer pair 1/4 still gives a couple of strong bands in the similar size range shown in Panel A.

### ***Limulus* and Sea Cucumber PCR with Consensus Primers**

Next, we tested our “con” primer pairs (designed against a consensus of fish and invertebrate EPN’s) using an annealing temperature of 37°C, however no primer set produced bands of the expected sizes (Figure 6).

## PCR with **CONSENSUS PRIMERS**

Annealing temp 37 °C, elongation 1min

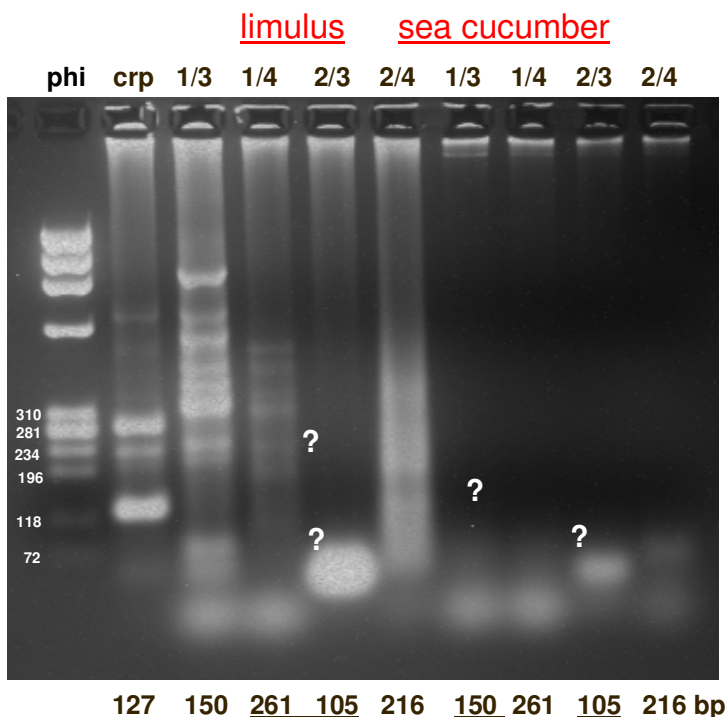


**Figure 6 - *Limulus* and Sea Cucumber PCR With Con 1-4 Primers.** The specific reaction conditions which earlier used to give 261mer and 105mer with sea primers (Figure 4 Panel B for *Limulus*, and Figure 5 Panel A for sea cucumber) did not give any similar results with con primers.

### ***Limulus* and Sea Cucumber PCR With 5-11 Primers**

We next tested our “5-11” primer pairs (designed exclusively against sequence domains totally conserved among the three known invertebrate EPN-like sequences) using a 37°C annealing temperature for sea cucumber DNA (Figure 7A) or *Limulus* DNA (Figure 7B). The strong “105mer” obtained using the 2/3 primer pair used *Limulus* DNA as a “positive control” since that reaction worked previously, but here the band migrates next to the 72 bp marker. This band has not been cloned yet. No amplicons of the expected sizes were obtained, but one primer

pair 6/10 produced a very strong band for both sea cucumber and *Limulus* DNA, although at different sizes. This band was subsequently cloned and sequenced, see below.

### PCR with 5-11 primers

-Primers designed against conserved regions between invertebrates-

**Sea cucumber, Annealing temp 37 °C, elongation 1 min**

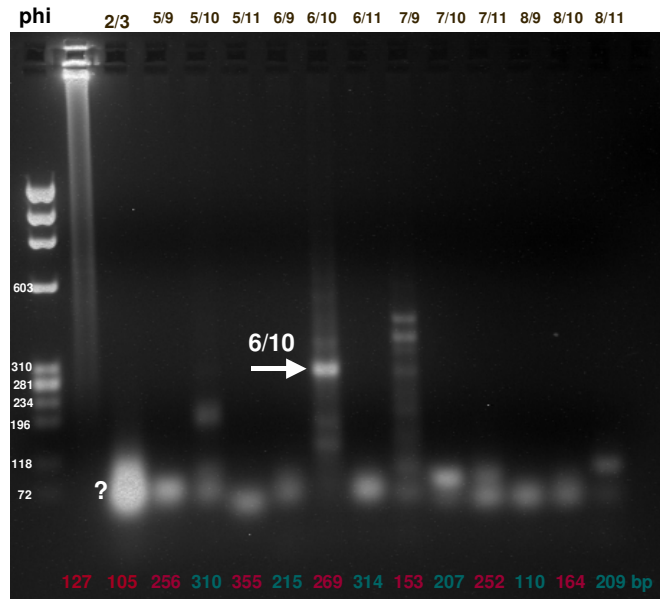


**Figure 7A- Sea Cucumber PCR Using 5-11 Primers.** None of the reactions produced amplicons of the expected sizes. A very strong amplicon with the 2/3 primer pair was amplified from *Limulus* DNA as a “positive control” based on previous experiments, but here it migrates slightly underneath the expected 105mer size. Note the strong band obtained using the 6/10 primer pair.

## PCR with 5-11 primers

*Limulus*, Annealing temp 37 °C, elongation 1 min

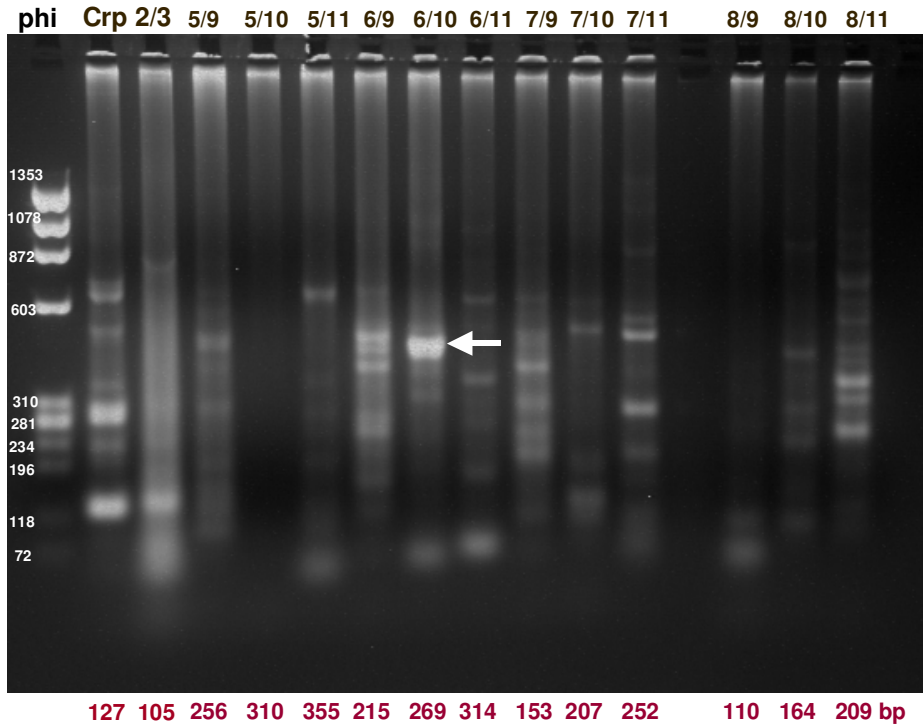


**Figure 7B - *Limulus* PCR Using 5-11 Primers.** No bands of the expected sizes were obtained. Again note the strong band using the 6/10 primer pair (white arrow).

In addition, PCR was performed for some *Limulus* housekeeper genes, including actin and GAPDH (Figure 8). Both of these reactions produced bands larger than the sizes predicted from *Limulus* cDNA sequences listed in Genbank, but this might be expected since we amplified from genomic DNA that might contain introns. Indeed this proved to be the case for the GAPDH band which was subsequently cloned and sequenced, see below.

## Limulus PCR 9-21-04

30 Cycles, 94C for 30 Sec, 55C for 30 Sec, 72C for 40 Sec

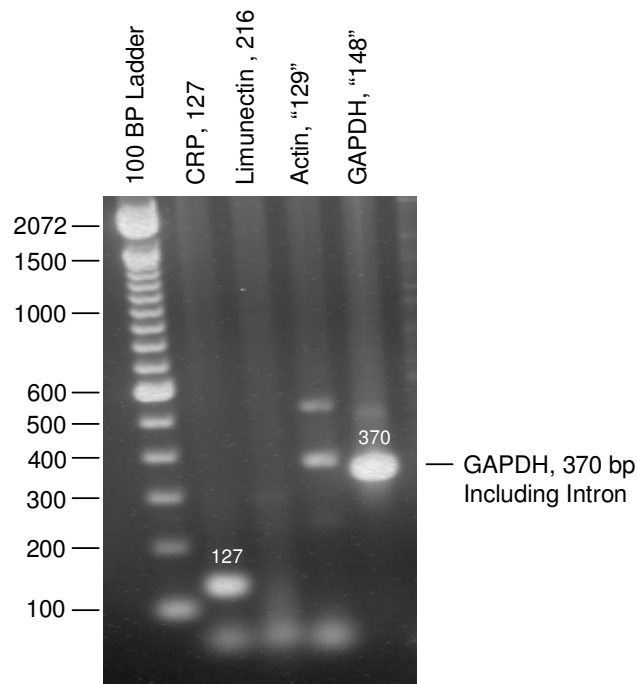


**Figure 8 – PCR of *Limulus* Housekeeper Genes.** Amplicons were observed for Actin and GAPDH, but were larger than the sizes predicted on the cDNA sizes in GenBank. The GAPDH band proved to be GAPDH upon cloning and sequencing with an added intron (Dave Adams, unpublished).

### Cloning and Sequencing Selected *Limulus* PCR Bands

Several different bands amplified from *Limulus* DNA using primers 6 and 10 were cloned by Dave Adams (WPI), and sequenced by the Umass Nucleic Acid Facility (Worcester). None of the sequences obtained showed any significant homology to the published vertebrate or invertebrate ependymin-like sequences when blasted against Genbank, including the very strong band at approximately 500 bp. However, one of the 6/10 bands at approximately 300 bp (clone-12) (seen in Figure 7B underneath the 500 bp band) showed very strong homology (88% over 292 bp) with mouse FGF-14 (Figure 9), known to induce neurogenesis in mouse (Smallwood *et*



The strong 370 bp band in the *Limulus* GAPDH reaction was also cloned and sequenced (Adams, unpublished) (Figure 10A). The 5' and 3' ends of this sequence align perfectly with the *Limulus* GAPDH cDNA in Genbank (Figure 10B), but the middle includes a genomic intron not found in the GenBank cDNA sequence.

## Cloned *Limulus* GAPDH

370 bp Fragment Amplified with Primers 1 and 2

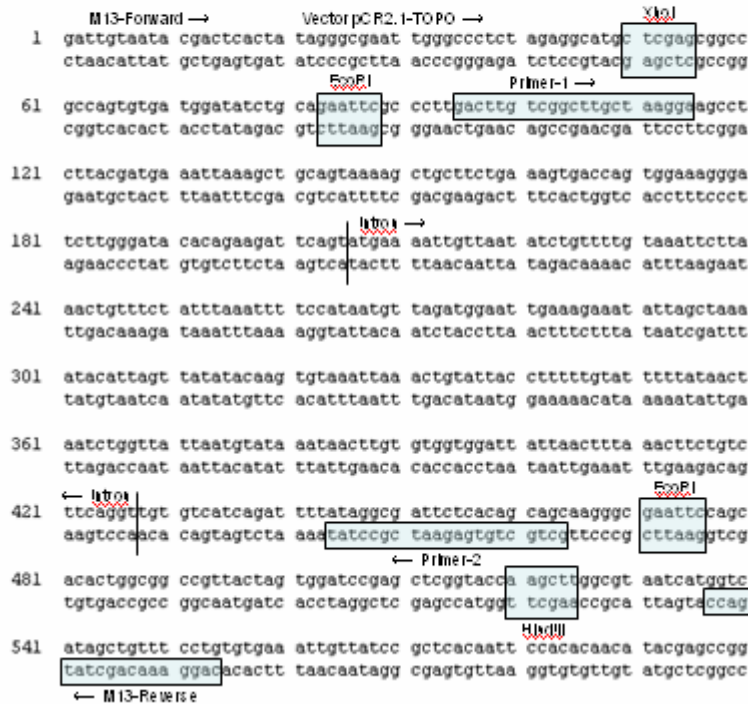


**Figure 10A – Sequence of *Limulus* GAPDH.** The 370 bp amplicon amplified by *Limulus* GAPDH primers from *Limulus* genomic DNA was cloned into plasmid pCR-2.1-TOPO (In vitrogen) by TA-cloning. It was then sequenced at the Umass Nucleic Acid Facility (Worcester) (Adams, unpublished).

## BLAST Alignment of Limulus Clone (Initial Exon) with GenBank Limulus GAPDH cDNA

```

 >gi|41394414|gb|AY522944.1 Limulus polyphemus glyceraldehyde 3-phosphate dehydrogenase (G3PDH)
      mRNA, partial cds
      Length = 891

Score = 220 bits (111), Expect = 2e-54
Identities = 111/111 (100%)
Strand = Plus / Plus

Query: 1  gacttgtcggccttgctaaggaagcctcttacgatgaaattaaagctgcagtaaaagctgc 60
          |||
Sbjct: 687 gacttgtcggccttgctaaggaagcctcttacgatgaaattaaagctgcagtaaaagctgc 746

Query: 61  ttctgaaagtgaccagtggaaggatcttgggatacacagaagattcagt 111
          |||
Sbjct: 747 ttctgaaagtgaccagtggaaggatcttgggatacacagaagattcagt 797

```

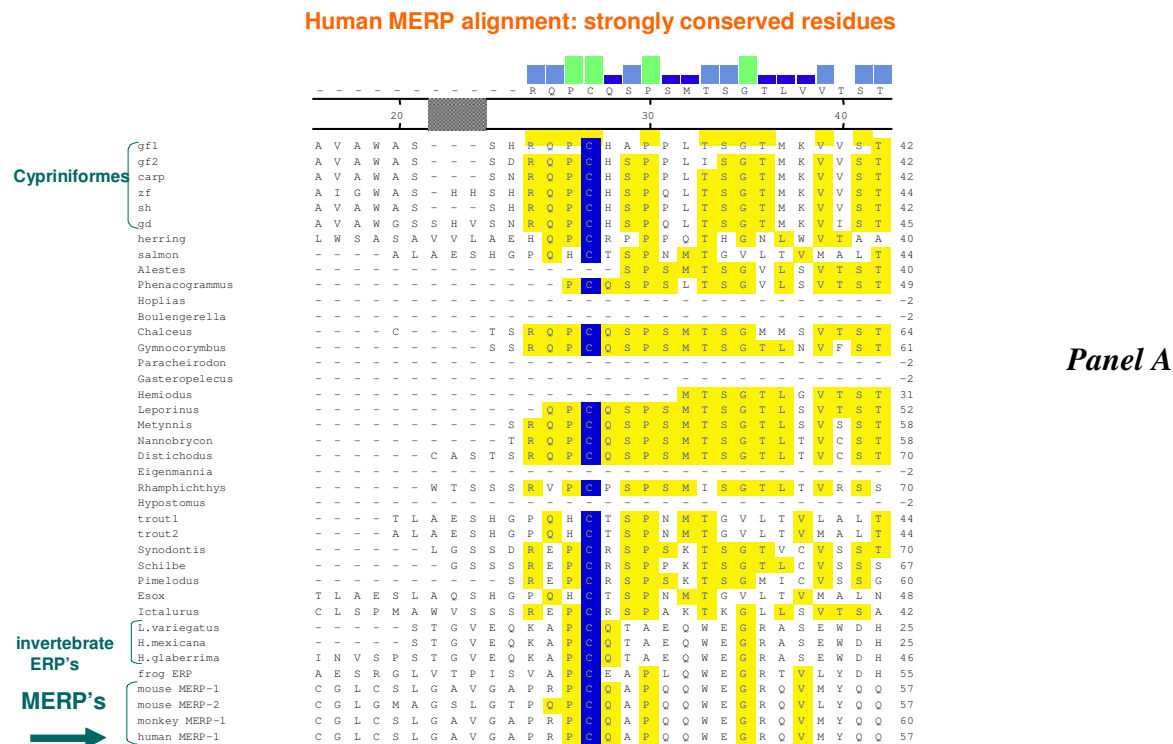
**Figure 10B – Alignment of *Limulus* Cloned GAPDH with the Genbank Entry for *Limulus* GAPDH.** Note that the alignment is perfect through position 111 on the clone, and thereafter it does not align. This is due to the presence of an intron in our genomic GAPDH clone missing in the Genbank cDNA entry.

## RESULTS: PART 2

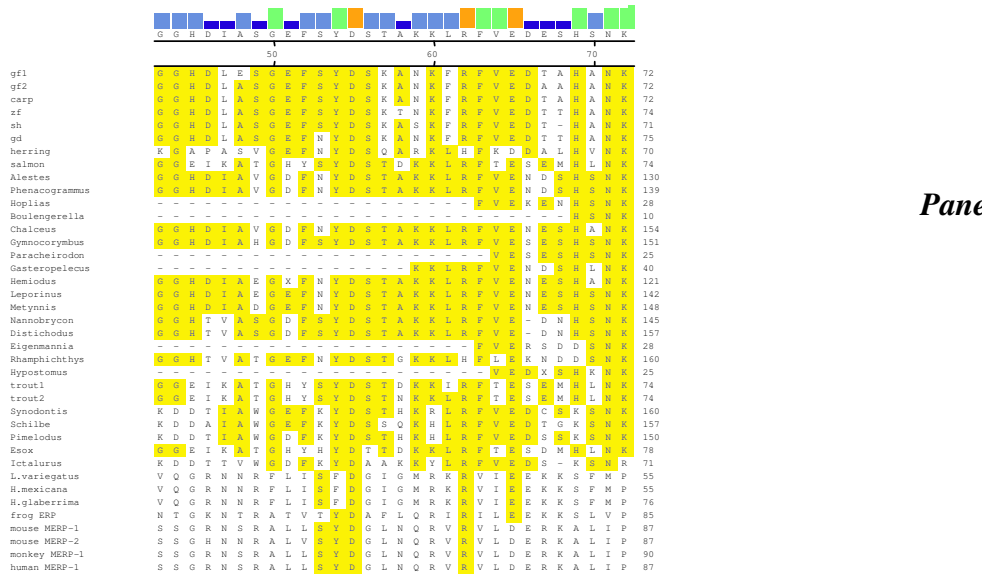
### “The Effects of a Human Ependymin Peptide on Human SHSY Neuroblastoma Cells”

#### Bioinformatics

A human homolog of ependymin has been identified, and its cDNA cloned (Apostolopoulos *et al.*, 2001). We used bioinformatics to compare the sequence of this mammalian ependymin-related protein (human MERP) to other ependymins and ependymin-related proteins, from invertebrates, teleosts, and mammals (Figure 11). The alignments show that human MERP shares four strongly conserved cysteine residues with all other ependymins and ERP's, as well as several leucine, tyrosine, and proline residues (shown as blue amino acids in the figure), and perfectly conserved tryptophan and glycine residues (red residues).

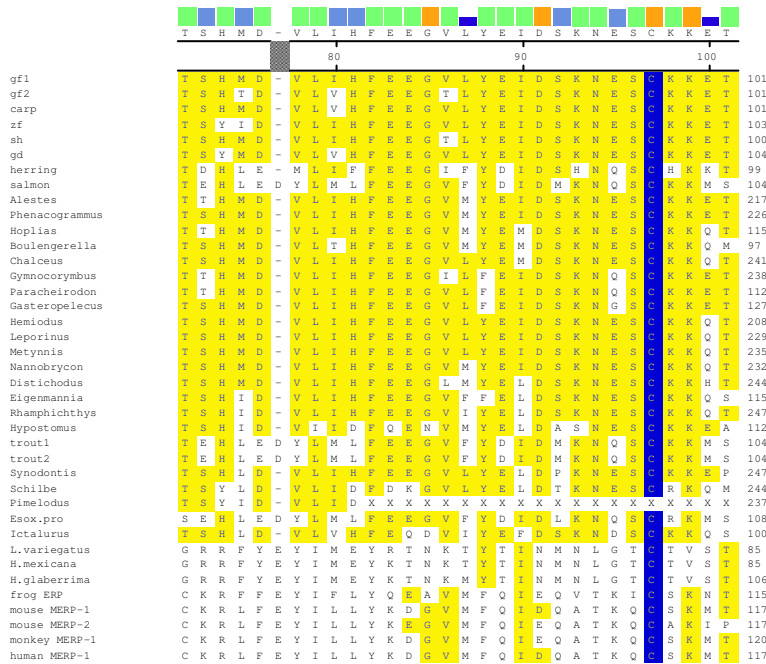


Human MERP alignment: strongly conserved residues



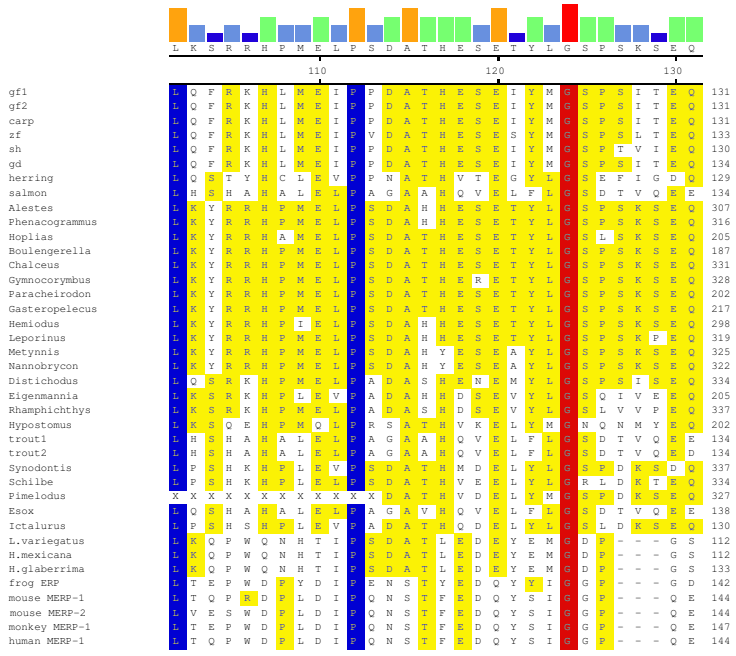
Panel B

Human MERP alignment: strongly conserved residues



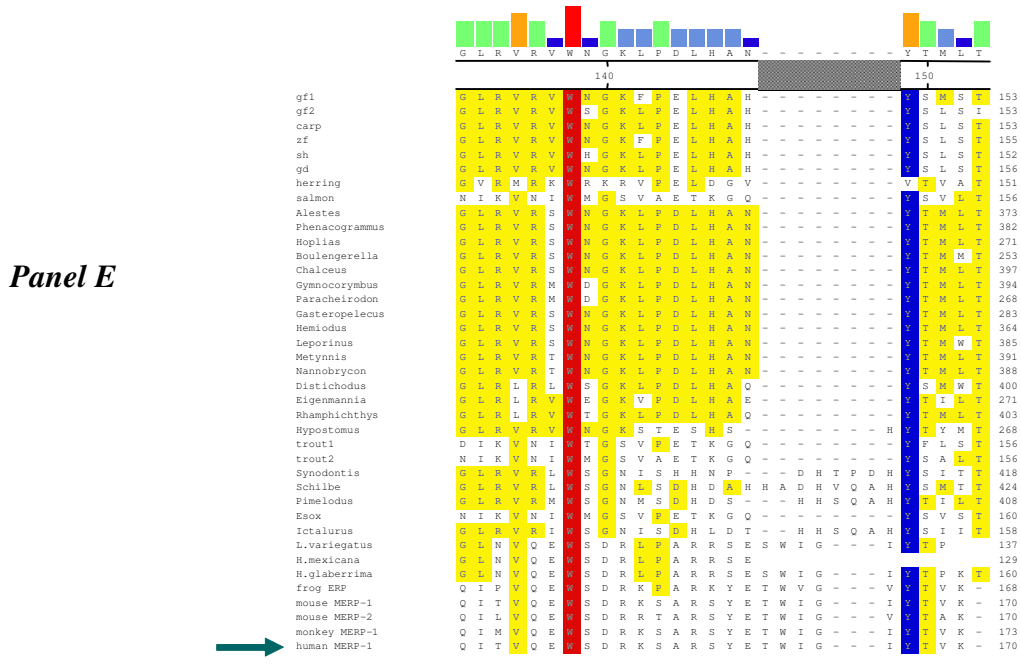
Panel C

Human MERP alignment: strongly conserved residues



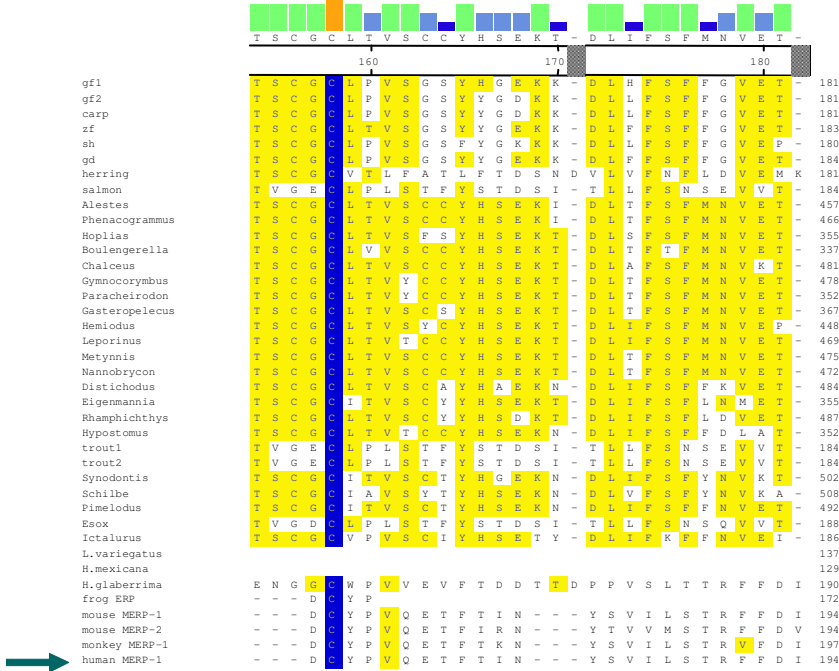
Panel D

Human MERP alignment: strongly conserved residues



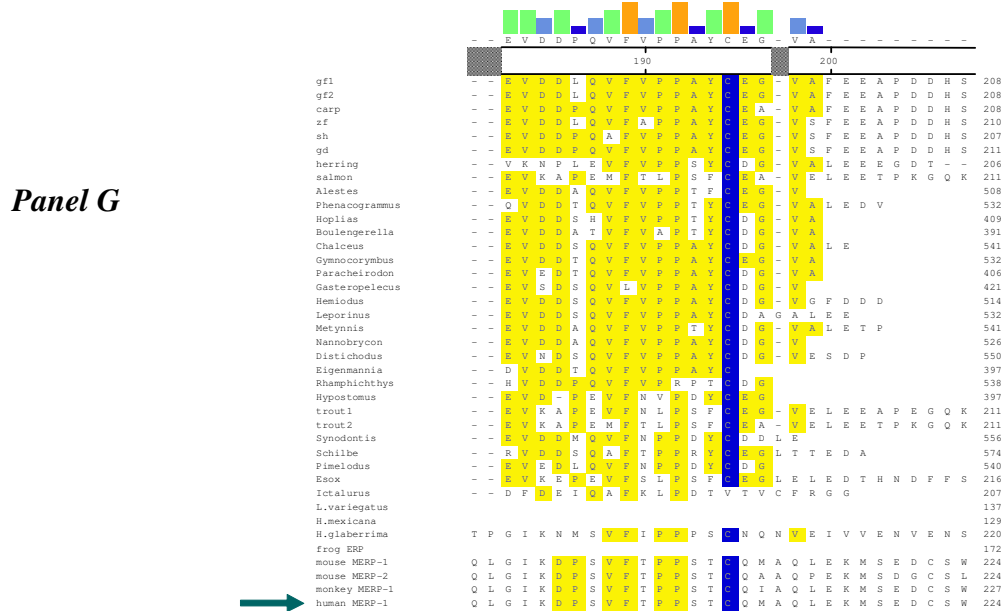
Panel E

Human MERP alignment: strongly conserved residues



Panel F

Human MERP alignment: strongly conserved residues



Panel G

Figure 11 - Bioinformatic Alignments of 39 Known Ependymin, or Ependymin Related Proteins Characterized to date. Four strongly conserved cysteine residues as well as leucine, tyrosine and proline residues are indicated in blue. Perfectly conserved glycine and tryptophan residues are indicated in red.

Based on the published human MERP sequence, we designed (Saif, 2004) a human peptide mimetic (hEPN-1) based on the analogous domain of goldfish mimetic CMX-8933 shown by our lab to be biologically active. The sequence of hEPN-1 is shown in Figure 12, and contains several highly conserved residues with teleost ependymins. CMX-8933 peptide itself was reproducibly generated when pure ependymin was incubated with trypsin. Since goldfish ECF is known to contain many proteases which might generate ependymin peptides, this particular peptide could represent a natural cleavage product of ependymin. Considering the mechanism of action of the CMX-8933 (Adams *et al.*, 2003), it could represent the receptor binding domain of ependymin.



**Figure 12 - hEPN-1 Peptide Derived from h-MERP 1.** The underlined hEPN-1 peptide sequence is shown relative to the analogous region of goldfish EPN-1 from where CMX-8933 was derived.

A 1 µg/ml treatment of mouse Neuro-2A cells with hEPN-1 for 24 hours was previously shown (Saif, 2004) to upregulate several growth-related genes by RT-PCR. We decided to test the biological activity of hEPN-1 against a human SHSY neuroblastoma cell line using RT-PCR.

### RT-PCR Analysis

SH-SY5Y human neuroblastoma cultures were treated with 1 µg/ml of hEPN-1 for 3 hours at 37°C, after which total cellular RNA was extracted for RT-PCR analysis. Figure 13 shows the RT-PCR results from control versus drug-treated cells. With the exception of the

GAPDH housekeeper control, each growth-related amplicon tested showed a stronger band in the drug-treated sample than the control. Table 2 below shows the summary of all the genes tested in this study along with their expected amplicon sizes based on the primers designed to retrieve them.

## Up-regulation of growth genes by h-epn 1 mimetics

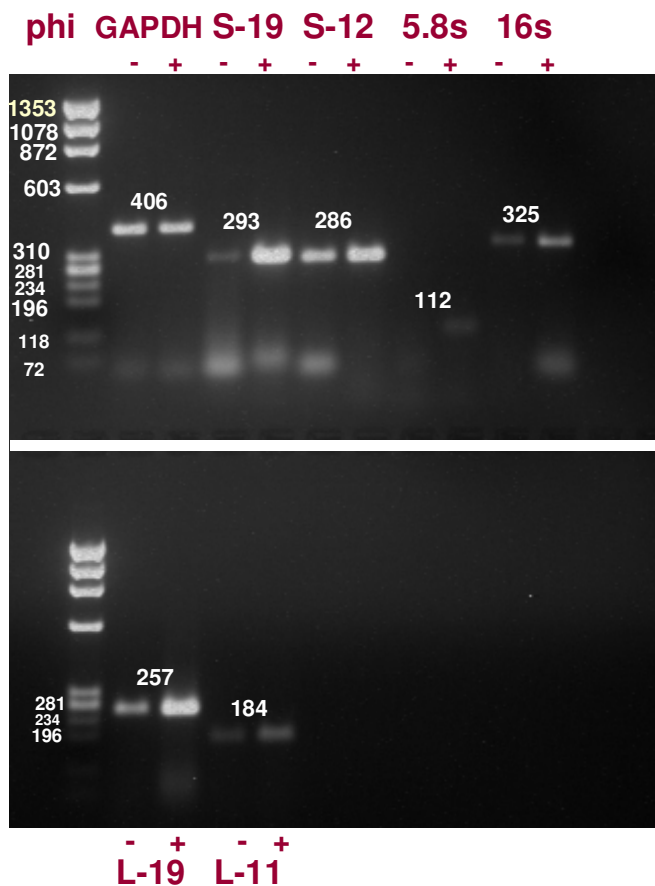


**Figure 13 - RT-PCR Analysis of Growth-Related Ribosomal Protein Genes from hEPN-1 Treated (+) and Control (-) SH-SY5Y Human Neuroblastoma Cells.** S-19, S-12, L-19 and L11 represent ribosomal proteins, while 5.8S and 16S represent nuclear and mitochondrial encoded ribosomal RNAs, respectively. The expected sizes in bp of each amplicon is denoted by white numbers.

Gene Tested	Site Encoded	Type	Expected Amplicon Size in bp
S-19	Nuclear	Ribosomal protein	293
S-12	Nuclear	Ribosomal protein	286
L-19	Nuclear	Ribosomal protein	257
L-11	Nuclear	Ribosomal protein	184
5.8S	Nuclear	Ribosomal RNA	112
16S	Mitochondrial	Ribosomal RNA	325

**Table 2 - Summary of Genes Tested and Their Expected Amplicon Sizes**

### Statistical Analysis of RT-PCR Data

Culture stimulation, RNA extraction, and RT-PCR procedures were repeated at least three more times. Fold upregulation values relative to untreated cultures were quantitated by SCION Image software (NIH). A histogram plot showing the mean fold upregulation for each amplicon is shown in Figure 14. Error bars denote one standard deviation. Statistically significant p-values (<0.05) (shown underneath each histogram in the figure) were obtained for the mean up-regulations of S-19, S-12, 5.8S and 16S genes, indicating hEPN-1 treatment of the human neuroblastoma cells indeed upregulates growth-related genes, as expected for a neurotrophic factor. Table 3 shows a summary of mean fold upregulation and corresponding p-values for each gene tested.

Gene Tested	Mean Fold Upregulation	p-value
S-19	2.76	<b>0.031</b>
S-12	1.74	<b>0.015</b>
L-19	2.38	0.058
L-11	1.30	0.083
5.8S	14.04	<b>0.018</b>
16S	3.91	<b>0.046</b>

**Table 3. Summary of Mean Fold Upregulation and Corresponding p-values.**  
The statistically significant p-values are indicated in bold.

## RT-PCR GENE UP-REGULATION DATA

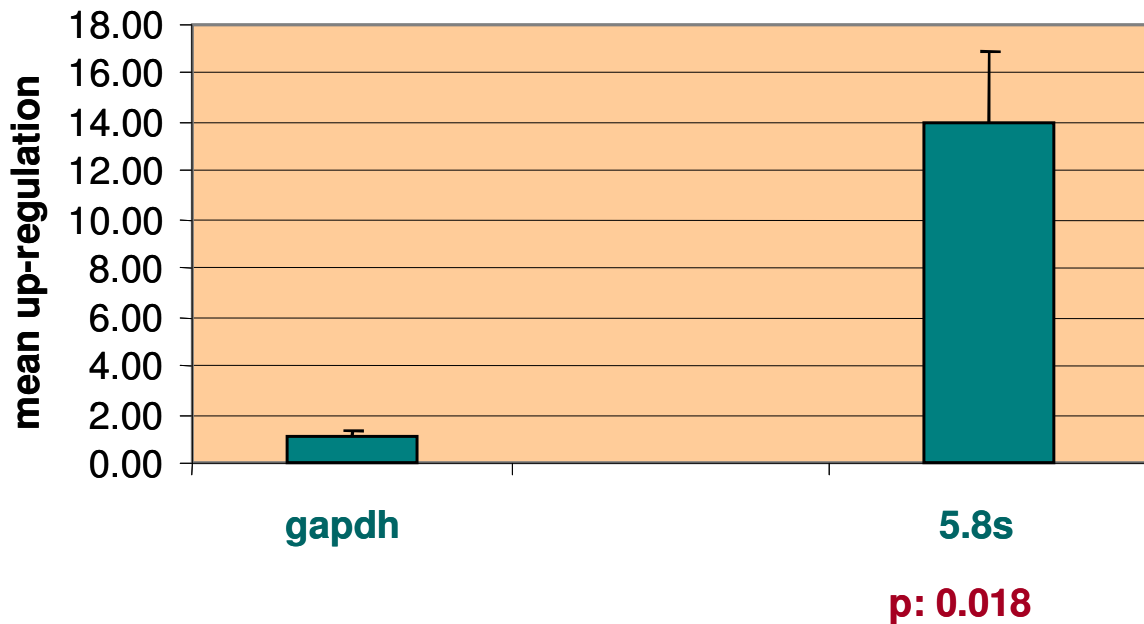
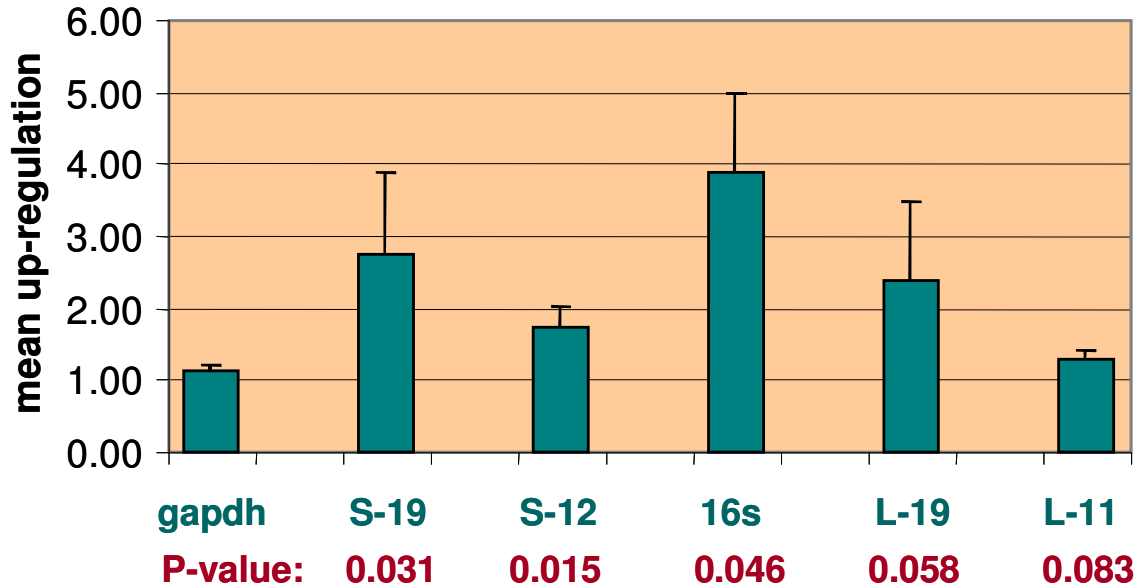


**Figure 14 – Quantitation of the Fold Upregulation of Growth-Related Genes Induced by hEPN-1.** The fold upregulation of specific RT-PCR amplicons in drug treated cultures relative to controls were quantitated by SCION Image software (NIH). Histograms represent the means of four independent experiments, while errorbars denote one standard deviation. p-values are shown beneath each histogram.

## DISCUSSION

### *PART 1 – Attempts to Clone Limulus Ependymin*

The purpose of part 1 of this thesis was to clone the *Limulus* ependymin (EPN) gene, or portions of it, to facilitate the assay of potential increases in its gene expression during leg regeneration. PCR was chosen as the cloning method based on our lab's previous successes using this technique to clone a variety of genes. *Limulus* sperm proved to be a rich source of genomic DNA, providing milligrams of material for analysis. The proteinase K/phenol extraction protocol used to isolate genomic DNA produced DNA pure enough, and intact enough, to produce successful PCR amplicons for positive controls GAPDH (proven by sequence analysis) and C-reactive protein (CRP).

For the EPN PCR, expected amplicons were achieved using EPN primers based on the published *H. glaberrima* sea cucumber ependymin-related sequence (Suarez-Castillo *et al.*, 2004) (sea primers) at various annealing temperatures, however these bands were not the strongest in a particular lane, and a number of non-specific bands were also observed. Using an annealing temperature of 37°C, and an elongation time of 1 min at 72°C was determined to be the optimum PCR conditions to produce the expected band sizes. Serial PCRs, in which a portion of a PCR reaction was used as template for a second PCR, helped to increase the *Limulus* amplicon masses. Raising the annealing temperature of the PCR, a strategy frequently used to help rid non-specific amplification, from 55°C to 58°C did not eliminate any extra bands. Interestingly, primer pair 1/3 which used to give a 150mer band at lower annealing temperatures appeared much weaker at this higher annealing temperature, so perhaps the primers to obtain this band were specific. To obtain more specific amplification in the future, higher annealing temperatures (i.e. 65°C) should be tested.

The second set of primers tested in this thesis was designed against a consensus of teleost and invertebrate ependymin and ependymin-related sequences (consensus primers) selecting the

nucleotide most frequently found at each position in several different conserved domains. Unfortunately, these consensus primers produced no *Limulus* amplicons of the expected sizes, even when using the optimum reaction conditions described above. These reaction conditions did however give bands of the expected sizes with sea primers for certain primer pairs (see underlined, Figure 6). Thus *Limulus* might have an EPN gene whose sequence more closely matches the sea cucumber *H. glaberrima* than an EPN consensus, especially for the domains analyzed here.

The third set of primers tested in this thesis was designed against domains totally conserved among the three known invertebrates (two sea cucumbers and a sea urchin). These primers are termed “5-11” (primer numbers 5 through 11). However, these primers also produced no bands of the expected sizes. Based on the expected size amplicons with the sea primers above, this was quite unexpected, because 5-11 primers also represent sequence identity with *H. glaberrima*. So perhaps *Limulus* EPN shows the most homology with *H. glaberrima* in the four domains tested, but the homology does not extend to the upstream regions where the primers 5-9 were designed (see Figure 3). Alternatively, these upstream regions in *Limulus* might contain introns to produce bands larger than the expected sizes based on the sea cucumber DNA (see Figure 7B, note multiple bands in certain lanes).

Interestingly, no EPN-related amplicons of the expected sizes could be obtained using consensus primers, or 5-11 conserved invertebrate primers against *Sclerodactyla briareus* sea cucumber DNA, except a “150mer” with *H. glaberrima* sea cucumber primers. Perhaps this is not so surprising given the extreme diversity of the sea cucumber family: The two sea cucumbers *Holothuria glaberrima* and *Sclerodactyla briareus* represent members of two different orders within the same class of animals. However, sea primers based on the *H. glaberrima* sequence seemed to work better against *Limulus* DNA, which belongs to a totally different phylum than the sea cucumbers.

Regarding the identification of specific PCR bands by cloning and sequencing, the strong *Limulus* GAPDH amplicon sequenced true (for those regions representing exons). A genomic GAPDH intron was identified for the first time in this study. This GAPDH amplicon provides a

housekeeper gene on which to base future growth-related gene comparisons. Several bands were cloned from the *Limulus* reaction with primers 6 and 10. The very strong band at around 500 bp (Figure 7B) aligned with no known ependymin, ependymin-related, or growth-related genes. However, the weaker band at 300 bp (found underneath the strong 500 bp band) showed a very strong homology to mouse fibroblast growth factor-14 (FGF-14). Interestingly, FGF-14 is known to have a role in nervous system development in mouse and is generally considered to be a subclass of neurotrophic factors (Smallwood *et al.*, 1996; Yamamoto *et al.*, 1998; Wang *et al.*, 2002). Future studies could involve the characterization of this FGF-like gene in *Limulus*, and its biological role in growth.

Future experiments may involve attempting to clone the *Limulus* EPN gene using RT-PCR from RNA isolated from regenerating leg tissue, since that RNA may be enriched for EPN transcripts. Degenerate primers (with two or more nucleotides at specific degenerate positions) could potentially be more useful than designing consensus primers. Non-PCR strategies may also be tested, including cDNA library screening.

## ***PART 2 - Human Ependymin Mimetic Appears to Elevate the Expression Levels of Growth-Related Genes in Human Neuroblastoma Cells***

The goal of the second part of this thesis was to determine whether treatment of cultured human SHSY neuroblastoma cells with peptide hEPN-1 upregulates the expression of growth-related genes. hEPN-1 is a small peptide whose sequence is based on a central domain of human mammalian ependymin-related protein (Apostolopoulos *et al.*, 2001) analogous to the region of goldfish EPN that CMX-8933 is designed against. Saif (2004) previously used RT-PCR to determine that hEPN-1 activates the expression of several growth-related genes in mouse neuroblastoma cells. Here, hEPN-1 was found to increase the expression of the nuclear genes encoding ribosomal proteins S-19 and S-12, an average of 2.76 fold and 1.74 fold, with statistically significant p-values of 0.031 and 0.015 (<0.05), respectively. The expression level of nuclear encoded 5.8S ribosomal RNA was also found to be increased an average of 14.04 fold, with a statistically significant p-value of 0.018. The mitochondrial encoded 16S ribosomal RNA was increased an average of 3.91 fold, with a p-value of 0.046. The mRNAs for ribosomal

proteins L-19 and L-11 did not produce significant p-values, however further data from independent observations could help achieve significance. Among the genes tested, only 5.8S did not produce the expected amplicon size with respect to our primers designed. In the future, this band could be cloned and sequenced to verify its composition .

Overall, the data from part-2 suggests that the human peptide indeed has biological activity in human cells, and might be involved in stimulating cell growth and division, a process which requires the increased expression of ribosomal RNA and proteins, a hallmark of proliferating cells (Angelastro *et al.*, 2002; Raska *et al.*, 2004). These genes were specifically chosen for assay due to their well known central roles in cell growth.

Future studies could analyze the expression of other growth-related genes, such as the upregulation of cell cycle proteins like cyclins, or the down-regulation of pro-apoptotic genes as possible indicators of cell proliferation. The growth factors are especially known for their abilities to induce early and late response genes in the G1 phase of the cell cycle. Such genes involve c-jun and c-fos early response genes or cdk 2,4,6 and cyclin D and E late response genes. These genes are therefore possible candidates to test the growth promoting abilities of the human peptide. Indeed, both h-EPN-1 and h-EPN-2 (the latter includes h-EPN-1 and 6 aa upstream of it) have been shown to upregulate the c-jun and c-fos mRNA levels (protein products of which constitute the AP-1 transcription factor) in mouse Neuro-2A cells (Saif, 2004). AP-1 is a transcription factor upstream of many genes involved in neuronal growth and synaptic plasticity (Sanyal *et al.*, 2002), and its downstream genes are therefore possible candidates for analysis, as well as AP-1 itself. For example, AP-1 is known to activate Nerve Growth Factor (NGF) and positively regulate the expression of cyclin D1 (Shaulian and Karin, 2001; 2002) and the anti apoptotic bcl-2 gene. AP-1's role in improving synaptic strength and number can not be underestimated since such outcomes are essential to re-constitute the 'lost' synaptic connections within CNS after neural injury, such as stroke. Therefore, genes regulating the process of synaptic plasticity are also worth testing in regards to the therapeutic function of our human mimetic. Genes known to be activated by other NTFs could also be studied (Greene *et al.*, 2000). For example, the components of AP-1 (c-Jun and c-Fos) are known to be activated by

nerve growth factor (NGF). Hybridization arrays or transcription factor arrays could be set up to study the gene expression induced by human EPN mimetics.

Our observed upregulations could be optimized by performing time-course and dose-response experiments. SY-SY5Y cells are known to have a generation time of 48 hours, so treating the cells for at least that long will make sure that every cell in the population will be exposed to the drug during one cell cycle. A different mimetic h-EPN-2 activity in SHSY cells could also be studied in a similar manner.

Since our lab's ultimate goal is to generate a drug that can be used in patients with neuro-pathological conditions, the mechanism of action of such a potential drug has to be fully understood. The mechanism of action of goldfish-based CMX-8933 has been investigated in our lab for several years in mouse neuroblastoma cells and rat primary neuronal cultures, and is known to involve protein kinase-C, protein tyrosine kinases, MEK kinase, and AP-1. It has also been proposed that the peptide could represent the receptor binding domain of ependymin. So it remains to be seen whether hEPN-1 uses similar mechanisms as that of CMX-8933, or whether it represents the receptor binding domain of human MERP-1. Alternatively, other peptides could be designed based on other domains of the human MERP sequence to see if different domains activate different pathways. Following the discovery of stem cells in adult brain tissue (Temple and Alvarez-Buylla 1999; Temple, 2001), the role of neurotrophic factors in stimulating their growth has been the center of attraction. In developing brain, NTF's are known to control the differentiation of neural stem cells, and similar mechanism is thought to occur following ischemic brain injury (Abe, 2000). So future experiments may involve assaying whether hEPN-1 activates adult neuronal stem cells.

Once the function and mechanism of action of hEPN-1 are more fully understood, its therapeutic applications in stroke patients could be explored, as was the therapeutic application of CMX-9236 for stroke (Shashoua *et al.*, 2003). Since neuro-pathological conditions such as stroke and neurodegenerative diseases involve an immense loss of neuronal function, a peptide stimulating the cell growth or aiding in the regeneration of nerve tissue could provide a useful strategy in the therapy of such pathological conditions.

## BIBLIOGRAPHY

- Abe K (2000) Therapeutic potential of neurotrophic factors and neural stem cells against ischemic brain injury. *J Cereb Blood Flow Metab* **10**: 1393-1408.
- Adams DS and Shashoua VE (1994) Cloning and sequencing the genes encoding goldfish and carp ependymin. *Gene* **141**: 237-241.
- Adams DS, Kiyokawa M, Getman M, Shashoua VE (1996) Genes encoding giant danio and golden shiner ependymin. *Neurochemical Research* **21(3)**: 377-384.
- Adams DS, Boyer-Boiteau A, Hasson B, El-Khisin, Shashoua VE (2003) A peptide fragment of ependymin neurotrophic factor uses PKC and the MAPK pathway to activate JNK and a functional AP-1 containing c-Jun and c-Fos proteins in mouse NB2a cells. *Journal of Neuroscience Research* **72**: 405-416.
- Anderson MJ, Choy CY, Waxman SG (1986) Self-organization of ependyma in regenerating teleost spinal cord: Evidence from serial section reconstructions. *Journal of Embryol. Exp. Morph.* **96**: 1-18.
- Angelastro JM , Torocsik B, Greene LA (2002) Nerve growth factor selectively regulates expression of transcripts encoding ribosomal proteins. *BMC Neuroscience* **3**:3.
- Apostolopoulos J, Sparrow RL, McLeod JL, Collier FM, Darcy PK, Slater HR, Ngu C, Gregorio-King CC, Kirkland MA (2001) Identification and characterization of a novel family of mammalian ependymin-related proteins (MERPs) in hematopoietic, nonhematopoietic, and malignant tissues. *DNA Cell Biology* **20**: 625-635.
- Baroffio, LC (2000) The role of ependymin in *Limulus polyphemus* limb regeneration. Major Qualifying Project BB-DVG 1848, Worcester Polytechnic Institute.
- Barroso GL (1999) Immunohistochemical Evidence for the Expression of Ependymin in *Limulus polyphemus*. WPI Master's Thesis, May 1999.
- Chan PH and Kawase M (1998) Overexpression of SOD1 in transgenic rats protects vulnerable neurons against ischemic damage after cerebral ischemia and reperfusion. *Journal of Neuroscience* **20**: 8292-8299.
- Chernoff EAG (1996) Spinal Cord Regeneration: a phenomenon unique to urodeles? *International Journal of Developmental Biology* **40**: 823-831.
- Chernoff EAG, Stocum DL, Nye HLD, Cameron JA (2003) Urodele spinal cord regeneration and related processes. *Developmental Dynamics* **226**: 295-307.

- Clare AS, Lumb G, Clare PA, Costlow JD (1990) A morphological study of wound response and telson regeneration in postlarval *Limulus polyphemus*. *Invertebrate Reproduction and Development* **17**(1): 77-87
- Connor B, Dragunow M (1998) The role of neuronal growth factors in neurodegenerative disorders of the human brain. *Brain Research Reviews* **27**: 1-39.
- Costigan J, Gallant J (2004) Horseshoe crab growth factors: Immunohistology. Major Qualifying Project, Worcester Polytechnic Institute.
- Cruikshank A, Faulkner N, Gosling J, Ingemi K, Vescio J (1993) Cloning and sequencing of ependymin. Major Qualifying Project, Worcester Polytechnic Institute.
- Egar M, Simpson SB, Singer M (1970) The growth and differentiation of the regenerating spinal cord of the lizard, *Anolis carolinensis*. *Journal of Morphology* **131**: 131-152.
- Gaiddon C, Loeffler JP, Larmet Y (1996) Brain-derived neurotrophic factor stimulates AP-1 and cyclic AMP-responsive element dependent transcriptional activity in central nervous system neurons. *Journal of Neurochemistry* **66**: 2279-2286.
- Ganss B, Hoffmann W (1993) Calcium binding to sialic acids and its effect on the conformation of ependymins. *European Journal of Biochemistry* **217**: 275-280.
- Garcia-Arraras JE, Greenberg MJ (2001) Visceral regeneration in Holothurians. *Microscopy Research and Technique* **55**: 438-451.
- Greene LA, Angelastro JM, Klimaschewski L, Tang S, Vitolo OV, Weissman TA, Donlin LT, Shelanski ML (2000) Identification of diverse nerve growth factor-regulated genes by serial analysis of gene expression (SAGE) profiling. *Proceedings of the National Academy of Sciences* **97** (19): 10424-10429.
- Gregorio-King CC, Mcleod JL, Collier F, Collier GR, Bolton KA, Van Der Meer GJ, Apostolopoulos J, Kirkland M (2002) MERP1: a mammalian ependymin-related protein gene differentially expressed in hematopoietic cells. *Gene* **286** (2): 249-257.
- Hefti F (1997) Pharmacology of neurotrophic factors. *Annual Review of Pharmacology and Toxicology* **37**: 239-267.
- Hoffmann W, Sterrer S, Konigstorfer A (1990) Biosynthesis and expression of ependymin homologous sequences in zebrafish brain. *Neuroscience* **37**: 277-84.
- Ikeda T, Xia XY, Xia YX, Ikenoue T, Han B, Choi BH (2000) Glial cell line-derived neurotrophic factor protects against ischemia/hypoxia-induced brain injury in neonatal rat. *Acta Neuropathologica* **100**: 161-167.

- Ip NY, Stitt TN, Tapley P, Klein R, Glass DJ, Fandl J, Greene LA, Barbacid M, Yancopoulos GD (1993) Similarities and differences in the way neurotrophins interact with the Trk receptors in neuronal and nonneuronal cells. *Neuron* **10**: 137-149.
- Johansson CB, Momma S, Clarke DL, Risling M, Lendahl U, Frisen J (1999) Identification of a neural stem cell in the adult mammalian central nervous system. *Cell* **96**: 25-43.
- Nimmrich I, Erdmann S, Melchers U, Chtarbova S, Finke U, Hentsch S, Hoffmann I, Oertel M, Hoffmann W, Muller O (2001) The novel ependymin related gene UCC1 is highly expressed in colorectal tumor cells. *Cancer Letters* **165 (1)**: 71-9.
- O'Hara CM, Egar MW, Chernoff EAG (1992) Re-organization of the ependyma during axolotl spinal cord regeneration: Changes in intermediate filament and fibronectin expression. *Developmental Dynamics* **193**: 103-115.
- Orti G, Meyer A (1996) Molecular evolution of ependymin and the phylogenetic resolution of early divergences among euteleost fishes. *Molecular Biology and Evolution* **13(4)**: 556-573.
- Patel MN and McNamara JO (1995) Selective enhancement of axonal branching of cultured dentate gyrus neurons by neurotrophic factors. *Neuroscience* **69**: 763-770.
- Raska I, Koberna K, Malinsky J, Fidlerova H, Masata M (2004) The nucleolus and transcription of ribosomal genes. *Biology of the Cell* **96**: 579-594.
- Saif, Sakina (2004) AP-1 is required for CMX-8933-induced SOD upregulation and is translocated in response to a human EPN mimetic. WPI Thesis, April, 2004.
- Sanyal S, Sandstrom DT, Hoeffler CA, Remaswami M (2002) AP-1 functions upstream of CREB to control synaptic plasticity in *Drosophila*. *Nature* **416**: 870-874.
- Schmidt JT, Schmidt R, Lin WC, Jian XY, Stuermer CA (1991) Ependymin as a substrate for outgrowth of axons from cultured explants of goldfish retina. *Journal of Neurobiology* **22(1)**: 40-54.
- Schmidt R (1995) Cell adhesion molecules in memory formation. *Behavioral Brain Research* **66**: 65-72.
- Shashoua VE (1976) Identification of specific changes on the pattern of brain protein synthesis after training. *Science* **193**: 1264-1266.
- Shashoua VE and Benowitz LI (1977) Localization of a brain protein metabolically linked with behavioral plasticity in the goldfish. *Brain Res* **136**: 227-242.
- Shashoua VE and Moore ME (1978) Effect of antisera to and goldfish brain proteins on the retention of a newly acquired behavior. *Brain Research* **148**: 441-449.

- Shashoua VE (1988) Monomeric and polymeric forms of ependymin: a brain extracellular glycoprotein implicated in memory consolidation processes. *Neurochemical Research* **13(7)**: 649-655.
- Shashoua VE, Schmidt JT (1988) Antibodies to ependymin block the sharpening of the regenerating retinotectal projection in goldfish. *Brain Research* **446**: 269-284.
- Shashoua VE, Hesse GW, Milinazzo B (1990) Evidence for the in vivo polymerization of ependymin: a brain extracellular glycoprotein. *Brain Research* **522(2)**: 181-190.
- Shashoua VE (1990) The role of ependymin in neuronal plasticity and LTP. *Advances in Experimental Medicine and Biology* **268**: 333-345.
- Shashoua VE (1991) Ependymin, a brain extracellular glycoprotein, and CNS plasticity. *Annals NY Academy of Science* **627**: 94-114.
- Shashoua VE, Adams DS, Boyer-Boiteau A (2003) Neuroprotective effects of a new synthetic peptide, CMX-9236, in *in vitro* and *in vivo* models of cerebral ischemia. *Brain Research* **936**: 214-223.
- Shashoua VE, Adams DS, Volodina NV, Lia H (2004) New synthetic peptides can enhance gene expression of key antioxidant defense enzymes *in vitro* and *in vivo*. *Brain Research* **1024**: 34-43.
- Shaulian E and Karin M (2001) AP-1 in cell proliferation and survival. *Oncogene* **20(19)**: 2390-2400.
- Shaulian E and Karin M (2002) AP-1 as a regulator of cell life and death. *Nature Cell Biology* **4(5)**:E131-136.
- Smallwood PM, Munoz-Sanjuan I, Tong P, Macke JP, Hendry SH, Gilbert DJ, Copeland NG, Jenkins NA and Nathans J (1996) Fibroblast growth factor (FGF) homologous factors: New members of the FGF family implicated in nervous system development. *Proc. Natl. Acad. Sci. U.S.A.* **93** (18): 9850-9857.
- Suarez-Castillo EC, Medina-Ortiz WE, Roig-Lopez JL, Garcia-Arraras JE (2004) Ependymin, a gene involved in regeneration and neuroplasticity in vertebrates, is overexpressed during regeneration in the echinoderm *Holothuria glaberrima*. *Gene* **334**:133-43.
- Temple S and Alvarez-Buylla A (1999) Stem cells in the adult mammalian central nervous system. *Curr. Opin. Neurobiol.* **9**: 135-141.
- Temple S (2001) The development of neural stem cells. *Nature* **414**: 112-117.

Wang Q, Bardgett ME, Wong M, Wozniak DF, Lou J, McNeil BD, Chen C, Nardi A, Reid DC, Yamada K and Ornitz DM (2002) Ataxia and paroxysmal dyskinesia in mice lacking axonally transported FGF14. *Neuron* 35 (1): 25-38.

Yamamoto S, Mikami T, Ohbayashi N, Ohta M and Itoh N (1998) Structure and expression of a novel isoform of mouse FGF homologous factor. *Biochim. Biophys. Acta* 1398: 38-41.